

# Oscillatory Motions and Parabolic Manifolds at Infinity in the Planar Circular Restricted Three Body Problem

Maciej J. Capiński<sup>1</sup>

*AGH University of Science and Technology, al. Mickiewicza 30, 30-059 Kraków, Poland*

Marcel Guardia<sup>2</sup>

*Universitat Politècnica de Catalunya, Departament de Matemàtiques & IMTECH, Pau Gargallo 14, Barcelona, Spain & Centre de Recerca Matemàtica, Campus de Bellaterra, Edifici C, Barcelona, Spain*

Pau Martín<sup>3</sup>

*Universitat Politècnica de Catalunya, Departament de Matemàtiques & IMTECH, Pau Gargallo 14, Barcelona, Spain & Centre de Recerca Matemàtica, Campus de Bellaterra, Edifici C, Barcelona, Spain*

Tere Seara<sup>4</sup>

*Universitat Politècnica de Catalunya, Departament de Matemàtiques & IMTECH, Pau Gargallo 14, Barcelona, Spain & Centre de Recerca Matemàtica, Campus de Bellaterra, Edifici C, Barcelona, Spain*

Piotr Zgliczyński<sup>5</sup>

*Jagiellonian University, ul. prof. Stanisława Łojasiewicza 6, 30-348 Kraków, Poland*

---

## Abstract

Consider the Restricted Planar Circular 3 Body Problem with both realistic mass ratio and Jacobi constant for the Sun-Jupiter pair. We prove the existence of all possible combinations of past and future final motions. In particular, we obtain the existence of oscillatory motions. All the constructed trajectories cross the orbit of Jupiter but avoid close encounters with it. The proof relies on the method of correctly aligned windows and is computer assisted.

*Keywords:* Celestial mechanics, oscillatory motions, parabolic invariant manifolds, computer assisted proofs.

---

<sup>1</sup>M. C. has been partially supported by the NCN grant 2018/29/B/ST1/00109

<sup>2</sup>M. G. has received funding from the European Research Council (ERC) under the European Union's Horizon 2020 research and innovation programme (grant agreement No 757802). M. G. is supported by the Catalan Institution for Research and Advanced Studies via an ICREA Academia Prize 2019.

<sup>3</sup>P. M. has been partially supported by the Spanish MINECO-FEDER Grant PGC2018-100928-B-I00 and the Catalan grant 2017SGR1049

<sup>4</sup>T. S. has been also partly supported by the Spanish MINECO-FEDER Grant PGC2018-098676-B-100 (AEI/FEDER/UE), the Catalan grant 2017SGR1049 and by the Catalan Institution for Research and Advanced Studies via an ICREA Academia Prize 2019.

<sup>5</sup>P. Z. has been partially supported by the NCN grant 2019/35/B/ST1/00655

## 1. Introduction

The planar circular restricted three body problem (PCR3BP) models the motion of a body of zero mass under the Newtonian gravitational force exerted by two bodies of masses  $\mu$  and  $1 - \mu$  which evolve in circular motion around their center of mass on the same plane. In rotating coordinates, if we denote by  $q \in \mathbb{R}^2$  the position of the zero mass body and  $p \in \mathbb{R}^2$  its associated momentum, the PCR3BP is a Hamiltonian system with respect to

$$H(q, p; \mu) = \frac{\|p\|^2}{2} - q_1 p_2 + q_2 p_1 - \frac{1 - \mu}{\|q + \mu\|} - \frac{\mu}{\|q - (1 - \mu)\|}. \quad (1)$$

Since the Hamiltonian is autonomous, it is a first integral which correspond to the Jacobi constant in non-rotating coordinates. (Often the Jacobi constant is defined as  $J = -2H$ ).

In the 1922, J. Chazy classified the possible final motions the massless body in the PCR3BP may possess [1] (see also [2]), that is, the possible “states” that  $q(t)$  may possess as  $t \rightarrow \pm\infty$ . They can be:

- $H^\pm$  (hyperbolic):  $\|q(t)\| \rightarrow \infty$  and  $\|\dot{q}(t)\| \rightarrow c > 0$  as  $t \rightarrow \pm\infty$ .
- $P^\pm$  (parabolic):  $\|q(t)\| \rightarrow \infty$  and  $\|\dot{q}(t)\| \rightarrow 0$  as  $t \rightarrow \pm\infty$ .
- $B^\pm$  (bounded):  $\limsup_{t \rightarrow \pm\infty} \|q\| < +\infty$ .
- $OS^\pm$  (oscillatory):  $\limsup_{t \rightarrow \pm\infty} \|q\| = +\infty$  and  $\liminf_{t \rightarrow \pm\infty} \|q\| < +\infty$ .

Examples of all these types of motion, except the oscillatory ones, were already known by Chazy.

Oscillatory motions were proven to exist for the first time by Sitnikov [3] in the 1960’s for the nowadays called *Sitnikov model*, which is a symmetric restricted spatial 3 body problem. Moreover he proved that one can construct orbits with any prescribed past and future final motions.

The approach by Sitnikov and by most of the subsequent references (see below) to construct oscillatory motions strongly rely on perturbative methods (see for instance [4, 5]). As a consequence, the motions obtained are either confined to “small” regions of the phase space or only exist in certain narrow ranges of some parameters.

The purpose of this paper is to develop techniques to prove such behaviors in *non-perturbative* regimes. These techniques will rely on Computer Assisted Proofs. This will allow to deal with physical ranges of parameters and regions of the phase space (that is regions “close to” the orbits of the Sun and Jupiter).

---

*Email addresses:* [maciej.capinski@agh.edu.pl](mailto:maciej.capinski@agh.edu.pl) (Maciej J. Capiński), [marcel.guardia@upc.edu](mailto:marcel.guardia@upc.edu) (Marcel Guardia), [p.martin@upc.edu](mailto:p.martin@upc.edu) (Pau Martín), [tere.m-seara@upc.edu](mailto:tere.m-seara@upc.edu) (Tere Seara), [umzglicz@cyf-kr.edu.pl](mailto:umzglicz@cyf-kr.edu.pl) (Piotr Zgliczyński)

We consider the PCR3BP and apply these techniques to prove the existence of any combination of past and future motions, including the oscillatory ones, for some explicitly given values of the mass parameter  $\mu$  and energy level  $H$  (equivalently for a given value of the Jacobi constant). More concretely, we consider  $\mu = 0.0009537$  which corresponds to the mass ratio for the pair Sun-Jupiter and  $H = -1$ .

**Theorem 1.** *Consider the PCR3BP, that is, (1) with  $\mu = 0.0009537$ . Then,*

$$X^+ \cap Y^- \cap \{H = -1\} \neq \emptyset,$$

where  $X, Y = H, P, B, OS$ .

In particular, for  $r_0 := 0.5002$ ,

- There exist trajectories  $(q(t), p(t))$  such that

$$\limsup_{t \rightarrow \pm\infty} \|q(t)\| = +\infty \quad \text{and} \quad \liminf_{t \rightarrow \pm\infty} \|q(t)\| \leq r_0. \quad (2)$$

- For every sufficiently large  $K \gg 1$ , there exists a periodic orbit  $(q(t), p(t))$  such that

$$\sup_{t \in \mathbb{R}} \|q(t)\| \geq K \quad \text{and} \quad \inf_{t \in \mathbb{R}} \|q(t)\| \leq r_0.$$

This theorem gives the possibility of combining any past and future final motions at a given energy level and with a realistic mass ratio. Moreover, Item 1 in the theorem implies that there exist oscillatory motions which reach points which are closer to the Sun than Jupiter. That is, these oscillatory orbits cross the orbit of Jupiter (but stay away from collision with it). Item 2 of the theorem gives the existence of periodic orbits of the PCR3BP (in the rotating frame) which encircle Jupiter and go very far from the primaries.

This result focuses on the energy level  $H = -1$  since it is far from the limit cases where oscillatory motions can be proven analytically (see [4, 5], where the value of  $-H$  needs to be taken sufficiently large). Our methodology can be applied also to different energy levels and there is nothing special about  $H = -1$ . (In fact, from our proof it follows that there are orbits with oscillatory motions at any energy level sufficiently close to  $H = -1$ .)

The analysis of final motions, and in particular of oscillatory motions, has drawn considerable attention in the last decades since the pioneering work by Sitnikov [3]. In 1968, Alekseev extended the results of Sitnikov constructing all possible combinations of future and past final motions (and thus oscillatory motions) for the full three body problem assuming the third mass is small enough [6].

Later, J. Moser [7] gave a new proof which related the existence of oscillatory motions to symbolic dynamics. His approach has been very influential and has been applied to different Restricted 3 Body Problems [8, 4, 5, 9] and, roughly speaking, it is also applied in the present paper. Moeckel has also proved the existence of oscillatory motions via symbolic dynamics for the three body problem relying on dynamics close to triple collision [10] (and therefore for sufficiently small total angular momentum). Oscillatory motions have been also constructed relying on other techniques closer to those of Arnold diffusion [11, 12].

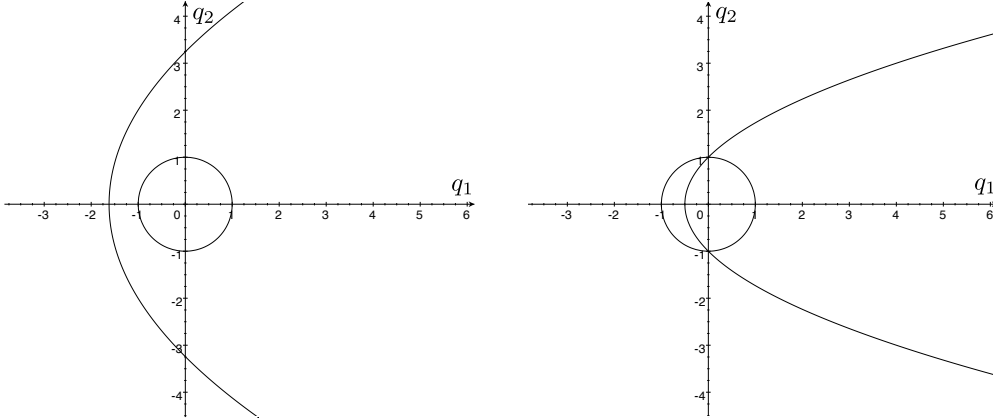


Figure 1: Parabolic motion from infinity for  $H = -1.8$  on the left (which is the case considered in [13, 14, 15]), and on the right for  $H = -1$  as is considered in the current paper. The circle represents the path of Jupiter and the Sun is positioned in the origin. The plots are for the limit case  $\mu = 0$ , but are very close to the trajectories in the Jupiter-Sun system.

Concerning the PCR3BP, [8] gives the existence of oscillatory motions and symbolic dynamics for arbitrarily large Jacobi constant assuming the mass ratio to be exponentially small with respect to the Jacobi constant. The paper [5] proved the result for any mass ratio and large enough Jacobi constant. As mentioned before, both references strongly rely on perturbative methods and only apply to nearly integrable regimes. Note that, in particular, the last result is *non-perturbative* with respect to the mass but requires large Jacobi constant which implies that the orbit are extremely far from the orbits of the Sun and Jupiter.

As far as the authors know, the only papers which deal with realistic values of both the mass ratio and energy level are [13, 14, 15] which are also computer assisted. Relying on completely different techniques from those of [7], Kaloshin and Galante construct trajectories whose initial conditions are “within the range of the Solar system” and become oscillatory as  $t \rightarrow +\infty$ . These orbits have energy  $H \leq -1.52$  (the needed conditions are rigorously verified with the aid of computers for  $H = -1.8$ ). See Figure 1 for the difference between their choice of energy and ours.

Not only the methods by Kaloshin and Galante are very different from ours, but also the orbits they construct are very different from those constructed in the present paper. In particular, their orbits undergo a drastic change in eccentricity whereas they stay away from the orbits of the primaries (note that the condition  $H \leq -1.52$  implies that the outer Hill region is disconnected from the inner ones). On the contrary, the oscillatory trajectories in the present paper have rather high eccentricity but can cross the trajectory of Jupiter.

### 1.1. The Moser approach and its implementation

Let us finish the introduction by explaining the approach that Moser developed to prove the existence of oscillatory motions for the Sitnikov problem and how his ideas are adapted in the present paper to prove Theorem 1.

The Sitnikov problem is a Hamiltonian system of one and a half degrees of freedom (one degree of freedom plus periodic time dependence). Let us denote it by  $\mathcal{H} = \mathcal{H}(q, \dot{q}, t)$  (its particular form is now not important). If one performs a suitable change of coordinates and considers the stroboscopic Poincaré map, the “parabolic infinity”  $q = +\infty, \dot{q} = 0$ , can be seen as a fixed point. The linearization of the stroboscopic map at this point is degenerate (equal to the identity).

The first step of Moser’s approach is to prove that, even if the fixed point is degenerate, it possesses one-dimensional stable and unstable invariant manifolds, which correspond to the parabolic orbits  $P^\pm$ . For the Sitnikov and the PCR3BP this fact had been proven previously in [16].

The second step is to prove that these invariant manifolds intersect transversally. This is the step which crucially relies on classical perturbative techniques such as Melnikov Theory [17] (as in [7, 8]) or singular perturbative techniques to deal with exponentially small phenomena (as in [5]).

If the fixed point at infinity was hyperbolic, a standard adaptation of Smale Theorem [18] (based on the classical Lambda Lemma) would lead to symbolic dynamics and oscillatory motions. However, since it is degenerate one needs to analyze carefully the dynamics close to the fixed point by a specific “parabolic Lambda lemma”.

In this paper, relying on the just explained Moser approach, we develop techniques which can be implemented in a computer to prove the existence of oscillatory motions.

First, in Section 3, we prove the existence of the local invariant manifolds and obtain quantitative estimates of its graph parameterizations. The approach, by using cone-shaped isolating blocks, is reminiscent to that of [16].

Then, in Sections 4 and 5, these techniques are applied to the PCR3BP. First, in Section 4, we perform several changes of coordinates to the PCR3BP so that it fits into the framework of Section 3. Then, in Section 5, we obtain estimates of the local invariant manifolds. In this section, we also extend them by the flow. This extension, computer assisted, is done in a way that one obtains fine rigorous estimates for the global invariant manifolds.

The fact that the infinity fixed point is degenerate implies that this computer implementation is by no means standard. Indeed, the dynamics in the invariant manifolds is extremely slow (its decay to the fixed point is polynomial in time instead of exponential).

The invariant manifolds intersect thanks to the Hamiltonian structure, and moreover, one can easily locate (some of) the intersections thanks to the reversibility of the PCR3BP with respect to the involution

$$(q_1, q_2, p_1, p_2) \rightarrow (q_1, -q_2, -p_1, p_2).$$

Our method does not require proving that the invariant manifolds intersect transversally. However, the method to construct oscillatory motions explained in the next paragraph implicitly relies on the fact that these invariant manifolds have intersections which are topologically transverse.

Finally, in Section 6, we use the methods of correctly aligned windows (covering relations) [19, 20, 21] to construct the motions described in Theorem 1. More precisely, we construct a sequence of windows which go from a small neighborhood of the fixed point at infinity to a neighborhood of one of the intersections between the stable and unstable invariant manifolds. Relying on the analysis of the local dynamics close to infinity in

Sections 4 and 5 and integrating with rigorous numerics the flow of the PCR3BP, we show that these windows are correctly aligned. Different choices of sequence of windows lead to different final motions. If one chooses a sequence such that (some of) the windows get closer and closer to the invariant manifolds of infinity, the orbits “hitting” this sequence of windows are oscillatory. On the contrary, if one chooses the windows uniformly away from the invariant manifolds (for instance one can take a fixed loop of correctly aligned windows), the corresponding orbits are bounded. Moreover, we also show that orbits passing through the edges of some of our windows lead to hyperbolic motions and that orbits reaching the parabolic stable/unstable manifolds lead to parabolic motions. From our topological construction it follows that we can link all these types of motions in forward and backward time.

## 2. Preliminaries

First we introduce some notation, which will be used throughout the paper. We write  $B_k$  for a open unit ball in  $\mathbb{R}^k$ , centered at zero, under some norm of our choice. (In our application we will use the max norm, but many of the arguments can be made norm independent.) We will write  $\bar{B}_k$  for the closure of  $B_k$ .

For a given norm  $\|\cdot\|$  on  $\mathbb{R}^n$  and for a matrix  $A \in \mathbb{R}^{n \times n}$  we define

$$\begin{aligned} m(A) &= \min_{p \in \mathbb{R}^n, \|p\|=1} \|Ap\|, \\ l(A) &= \lim_{h \rightarrow 0^+} \frac{\|\text{Id} + hA\| - \|\text{Id}\|}{h}, \\ m_l(A) &= \lim_{h \rightarrow 0^+} \frac{m(\text{Id} + hA) - \|\text{Id}\|}{h}. \end{aligned} \tag{3}$$

The  $l(A)$  is the logarithmic norm of  $A$  [22, 23]. It is known that  $l(A)$  is a convex function. The number  $m(A)$  is useful to us since it can be used to obtain the lower bound  $\|Ap\| \geq m(A) \|p\|$ . The number  $m_l(A)$  can be thought of as a ‘lower bound version’ of the logarithmic norm.

If  $s > 0$ , then

$$l(sA) = sl(A), \quad m_l(sA) = sm_l(A).$$

**Lemma 2** ([24]). *We have*

$$m(A) = \begin{cases} \frac{1}{\|A^{-1}\|} & \text{if } \det A \neq 0, \\ 0 & \text{otherwise,} \end{cases} \quad m_l(A) = -l(-A).$$

We now give two technical lemmas that allow us to obtain upper and lower bounds on  $l$  and  $m_l$ , respectively, for a weighted average of a family of matrices.

**Lemma 3.** *Let  $h : [0, 1] \rightarrow \mathbb{R}_+$  be a continuous function and let  $A : [0, 1] \rightarrow \mathbb{R}^{n \times n}$  be a measurable function such that  $l(A(s)) \leq L$  for  $s \in [0, 1]$ . Then*

$$l\left(\int_0^1 h(s) A(s) ds\right) \leq L \int_0^1 h(s) ds.$$

**Proof.** From Jensen's inequality applied to the convex function  $l$  we obtain

$$l\left(\int_0^1 h(s)A(s)ds\right) \leq \int_0^1 l(h(s)A(s))ds = \int_0^1 h(s)l(A(s))ds \leq L \int_0^1 h(s)ds,$$

as required. ■

**Lemma 4.** Let  $h : [0, 1] \rightarrow \mathbb{R}_+$  be a continuous function and let  $A : [0, 1] \rightarrow \mathbb{R}^{n \times n}$  be a measurable function such that  $m_l(A(s)) \geq M$  for  $s \in [0, 1]$ . Then

$$m_l\left(\int_0^1 h(s)A(s)ds\right) \geq M \int_0^1 h(s)ds.$$

**Proof.** Since  $A \mapsto l(-A)$  is convex,  $m_l(A) = -l(-A)$  is concave, so from Jensen's inequality

$$\begin{aligned} m_l\left(\int_0^1 h(s)A(s)ds\right) &\geq \int_0^1 m_l(h(s)A(s))ds \\ &= \int_0^1 h(s)m_l(A(s))ds \geq M \int_0^1 h(s)ds, \end{aligned}$$

as required. ■

### 3. Topologically hyperbolic manifolds

Let  $\Lambda$  be a smooth compact  $c$ -dimensional manifold without boundary. We will consider a vector field

$$F : \mathbb{R}^u \times \mathbb{R}^s \times \Lambda \rightarrow \mathbb{R}^u \times \mathbb{R}^s \times T\Lambda$$

(here  $T\Lambda$  is the tangent space) and an ODE

$$p' = F(p). \tag{4}$$

We shall write  $\Phi_t$  for the flow induced by (4). We shall assume that

$$\tilde{\Lambda} = \{(0, 0)\} \times \Lambda$$

is invariant under the flow. We will be in the context where for  $p \in \tilde{\Lambda}$  the derivative  $DF(p)$  can be zero.

The objective of this section will be to provide sufficient conditions for the existence and the construction of stable and unstable manifolds of  $\tilde{\Lambda}$ .

Let us introduce the following notation for coordinates:  $x \in \mathbb{R}^u$ ,  $y \in \mathbb{R}^s$ ,  $\lambda \in \Lambda$ . The coordinate  $x$  is towards the expanding direction,  $y$  is towards the contracting direction and  $\lambda$  is the center direction. We do not need to assume though that the coordinates  $x$  and  $y$  are perfectly aligned with the unstable and stable bundles of our system, respectively. A 'rough alignment' will turn out good enough, provided that the conditions needed for our construction are fulfilled.

Let  $L \in (0, 1]$  be a fixed constant, let  $\beta_u \subset \{1, \dots, u\}$ ,  $\beta_s \subset \{1, \dots, s\}$  (the sets  $\beta_u, \beta_s$  can be empty) and consider the following sets

$$\begin{aligned} S^u &= S_L^u = \{(x, y, \lambda) : \lambda \in \Lambda, \|y\| < L \|x\|, \|x\| < 1, x_i > 0 \text{ for } i \in \beta_u\}, \\ S^s &= S_L^s = \{(x, y, \lambda) : \lambda \in \Lambda, \|x\| < L \|y\|, \|y\| < 1, y_i > 0 \text{ for } i \in \beta_s\}. \end{aligned}$$

We define

$$\begin{aligned} S_-^u &= \{(x, y, \lambda) \in \overline{S^u} : \|x\| = 1 \text{ or } x_i = 0 \text{ for some } i \in \beta_u\}, \\ S_-^s &= \{(x, y, \lambda) \in \overline{S^s} : \|y\| = 1 \text{ or } y_i = 0 \text{ for some } i \in \beta_s\}. \end{aligned}$$

We shall refer to  $S_-^u, S_-^s$  as *exit sets*. We also define

$$\begin{aligned} S_+^u &= \{(x, y, \lambda) \in \overline{S^u} : \|y\| = L \|x\| \text{ and } \|x\| < 1\}, \\ S_+^s &= \{(x, y, \lambda) \in \overline{S^s} : \|x\| = L \|y\| \text{ and } \|y\| < 1\}. \end{aligned}$$

We shall refer to  $S_+^u, S_+^s$  as *entry sets*. Note that

$$\partial S^u = S_-^u \cup S_+^u \quad \text{and} \quad \partial S^s = S_-^s \cup S_+^s.$$

**Definition 5.** We say that  $S^u$  is an unstable sector if for every  $p \in S^u$  the forward trajectory leaves  $S^u$  through  $S_-^u$  and enters through  $S_+^u$ . More precisely, if the following two conditions are satisfied:

1. If  $p \in S^u$  then  $\Phi_{[0,t]}(p) \notin S^u$  for some  $t > 0$ ,
2. If  $p \in S_+^u$  then  $\Phi_{(0,t]}(p) \in S^u$  for some  $t > 0$ .

**Definition 6.** We say that  $S^s$  is a stable sector, if it is a unstable sector for the flow with reversed time.

The sets  $S^u$  and  $S^s$  will provide bounds for the domains in which the manifolds are positioned. To simplify the statements, we will sometimes refer to  $S^u$  and  $S^s$  as sectors.

**Remark 7.** Depending on the particular system the sets  $\beta_u, \beta_s$  can be empty. We consider them since in the equations of the PRC3BP at infinity, some of the coordinates will only have physical meaning when they are greater or equal to zero.

**Definition 8.** We will define the unstable and stable sets as

$$\begin{aligned} W^u(\tilde{\Lambda}) &= \left\{ p \in S^u : \Phi_t(p) \in S^u \text{ for } t \in (-\infty, 0] \text{ and } \lim_{t \rightarrow -\infty} \text{dist}(\Phi_t(p), \tilde{\Lambda}) = 0 \right\}, \\ W^s(\tilde{\Lambda}) &= \left\{ p \in S^s : \Phi_t(p) \in S^s \text{ for } t \in [0, +\infty) \text{ and } \lim_{t \rightarrow +\infty} \text{dist}(\Phi_t(p), \tilde{\Lambda}) = 0 \right\}, \end{aligned}$$

respectively.

In our work we will present tools which will allow us to establish the existence of unstable and stable sets which are graphs of Lipschitz functions

$$\begin{aligned} w^u &: \pi_{x,\lambda} S^u \rightarrow S^u, \\ w^s &: \pi_{y,\lambda} S^s \rightarrow S^s, \end{aligned}$$

$$W^u(\tilde{\Lambda}) = \text{graph}(w^u) = w^u(\pi_{x,\lambda}S^u), \quad W^s(\tilde{\Lambda}) = \text{graph}(w^s) = w^s(\pi_{y,\lambda}S^s),$$

where  $w^u, w^s$  satisfy

$$\pi_{x,\lambda}w^u(x, \lambda) = (x, \lambda), \quad \pi_{y,\lambda}w^s(y, \lambda) = (y, \lambda).$$

This will in particular mean that  $W^u(\tilde{\Lambda})$  and  $W^s(\tilde{\Lambda})$  are Lipschitz manifolds.

We now define what we will mean by saying that  $\tilde{\Lambda}$  is a *topologically hyperbolic* manifold.

**Definition 9.** *Assume that the unstable and stable sets are manifolds. If we have a neighbourhood  $U$  of  $\tilde{\Lambda}$  in which all points whose forward trajectories remain in  $U$  are in  $W^s(\tilde{\Lambda})$ , and all points from  $U$  whose backward trajectories remain in  $U$  are contained in  $W^u(\tilde{\Lambda})$ , then we call  $\tilde{\Lambda}$  a topologically hyperbolic manifold.*

We will be working under the assumption that in  $S^u$  and  $S^s$  we can factor out suitable terms from the derivative of  $F$ . From now on let us focus on the sector  $S^u$  within which we will establish the existence of the manifold  $W^u(\tilde{\Lambda})$ . (The results for  $W^s(\tilde{\Lambda})$  within  $S^s$  will follow by reversing the sign of the vector field, and swapping the roles of the coordinates  $x, y$ .)

For the factorisation of the suitable terms in  $S^u$  we will assume that there exist functions  $h : S^u \rightarrow \mathbb{R}$  and  $G : S^u \rightarrow \mathcal{L}(\mathbb{R}^u \times \mathbb{R}^s \times T\Lambda)$ , (here  $\mathcal{L}(X)$  stands for the space of Linear operators on  $X$ ), such that

$$h(x, y, \lambda) > 0, \quad \text{for all } (x, y, \lambda) \in S^u, \quad (5)$$

and

$$DF(x, y, \lambda) = h(x, y, \lambda)G(x, y, \lambda). \quad (6)$$

**Remark 10.** *Note that we allow  $h = 0$  on  $\tilde{\Lambda}$ . We also note that the case of (4–6) is fundamentally different from considering the case where we have an ODE with a vector field  $F(p) = h(p)g(p)$  and where  $h > 0$  and  $g$  has a NHIM. The latter case is trivial since the NHIM for  $g$  and its associated stable and unstable manifolds become invariant manifolds for  $F$  by a simple rescaling of time.*

Our objective will be to impose some normally-hyperbolic-type conditions on  $G$  in (6), from which we will be able to deduce the existence  $W^u(\tilde{\Lambda})$  in  $S^u$ . Our methods will lead to establishing the existence of the function  $w^u$ , which will be Lipschitz. They can be applied in a more general context, but to simplify the arguments we restrict to the case where  $\Lambda$  is a  $c$ -dimensional torus  $\Lambda = \mathbb{S}^c = (\mathbb{R}/(\text{mod } 2\pi))^c$ . Then we are in a convenient situation, since we have a covering

$$\varphi : \mathbb{R}^c \rightarrow (\mathbb{R}/(\text{mod } 2\pi))^c, \quad (7)$$

which gives us local charts as restrictions of  $\varphi$  to balls, provided that the radius of such balls is smaller than  $\pi$ .

### 3.1. Cone conditions and outflowing along cones

Let  $L_u, L_{cu}, L_s, L_{cs} > 0$

$$Q_u, Q_{cu}, Q_s, Q_{cs} : \mathbb{R}^{u+s+c} \rightarrow \mathbb{R}, \quad (8)$$

defined as

$$\begin{aligned} Q_u(x, y, \lambda) &:= L_u \|x\| - \|(y, \lambda)\|, \\ Q_{cu}(x, y, \lambda) &:= L_{cu} \|(x, \lambda)\| - \|y\|, \\ Q_s(x, y, \lambda) &:= L_s \|y\| - \|(x, \lambda)\|, \\ Q_{cs}(x, y, \lambda) &:= L_{cs} \|(y, \lambda)\| - \|x\|, \end{aligned}$$

We slightly abuse notations by referring to  $Q_u, Q_{cu}, Q_s$  and  $Q_{cs}$  as cones. We do so since for any point  $p \in \mathbb{R}^{u+s+c}$  the sets

$$Q_\kappa^+(p) := \{q : Q_\kappa(p - q) \geq 0\}, \quad \kappa \in \{u, cu, s, cs\}$$

are cones centered at  $p$ . (See Figure 2.) This means that  $Q_u, Q_{cu}, Q_s$  and  $Q_{cs}$  define cones that can be attached to any point  $p \in \mathbb{R}^{u+s+c}$ .

We will assume that  $L_s, L_u \in (0, \pi)$ . We do so for convenience: We are working in the simplified setting where  $\Lambda$  is a torus  $(\mathbb{R}/(2\pi))^c$ . When  $L_u \in (0, \pi)$  and  $p \in S^{cs}$ , then the set  $Q_u^+(p) \cap S^{cs}$  is contained in a single chart, since for any  $q \in Q_u^+(p)$  with  $\|\pi_x q\| \leq 1$  and  $\|\pi_y q\| \leq 1$  we will have

$$\|\pi_\theta(q - p)\| \leq \|\pi_{y,\theta}(q - p)\| \leq L_u \|\pi_x(q - p)\| \leq L_u (\|\pi_x q\| + \|\pi_x p\|) \leq 2L_u < 2\pi.$$

A mirror argument can be made that for  $p \in S^{cu}$  the set  $Q_s^+(p) \cap S^{cu}$  is also contained in a single chart.

We note though that for a given point  $p \in S^{cu}$  the set  $Q_{cu}^+(p)$  is only locally defined in a neighbourhood of  $p$ , which is small enough to be contained in a single chart. The same is for  $Q_{cs}^+(p)$ .

**Remark 11.** Whenever we write  $Q_{cu}(p - q)$  or  $Q_{cs}(p - q)$  we implicitly assume that  $q$  and  $p$  are in some common local chart.

**Definition 12.** Let  $U \subset \mathbb{R}^{u+s+c}$  and let  $\kappa \in \{u, cu\}$ . We say that a flow  $\Phi_t$  satisfies (forward)  $Q_\kappa$ -cone conditions in  $U$  if for every  $p_1, p_2 \in U$  satisfying  $Q_\kappa(p_1 - p_2) \geq 0$  the fact that  $\Phi_{[0,t]}(p_i) \subset U$ , for both  $i = 1, 2$  and some  $t > 0$ , implies that

$$Q_\kappa(\Phi_t(p_1) - \Phi_t(p_2)) \geq 0.$$

**Definition 13.** Let  $U \subset \mathbb{R}^{u+s+c}$  and let  $\kappa \in \{s, cs\}$ . We say that a flow  $\Phi_t$  satisfies (backward)  $Q_\kappa$ -cone conditions in  $U$  if for every  $p_1, p_2 \in U$  satisfying  $Q_\kappa(p_1 - p_2) \geq 0$  the fact that  $\Phi_{[-t,0]}(p_i) \subset U$ , for both  $i = 1, 2$  and some  $t > 0$ , implies that

$$Q_\kappa(\Phi_{-t}(p_1) - \Phi_{-t}(p_2)) \geq 0.$$

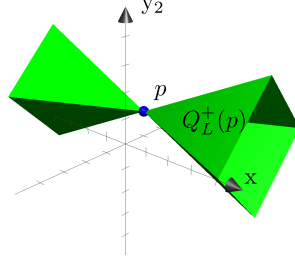


Figure 2: A cone attached at  $p = (0, 1, 1)$ , in the case when  $n_1 = 1$ ,  $n_2 = 2$ ,  $L = \frac{1}{2}$ ,  $\|x_1\| = |x_1|$  and  $\|y\| = \|(y_1, y_2)\| = |y_1| + |y_2|$ .

**Definition 14.** We say that  $\Phi_t$  is (forward) outflowing from  $S^{cs}$  along  $Q_u$  if for every  $p_1, p_2 \in S^{cs}$  satisfying  $Q_u(p_1 - p_2) \geq 0$  there exists a  $t > 0$  such that

$$\Phi_t(p_i) \notin S^{cs} \quad \text{for some } i \in \{1, 2\}.$$

**Definition 15.** We say that  $\Phi_t$  is (backward) outflowing from  $S^{cu}$  along  $Q_s$  if for every  $p_1, p_2 \in S^{cu}$  satisfying  $Q_s(p_1 - p_2) \geq 0$  there exists a  $t > 0$  such that

$$\Phi_{-t}(p_i) \notin S^{cu} \quad \text{for some } i \in \{1, 2\}.$$

Intuitively, if  $\Phi_t$  satisfies cone conditions then any two points which are aligned by the cones will flow to points, which are also aligned by the cones. The outflowing condition states that at least one of two such points will eventually flow out of the considered set.

### 3.2. Construction of stable and unstable manifolds

The aim of this section is to prove the following two theorems.

**Theorem 16.** Let  $S^u$  be a sector (see Definition 5) and denote by  $\Phi_t$  the flow induced by  $F$ . Assume that:

1. The flow  $\Phi_t$  satisfies forward cone conditions for  $Q_{cu}$  in  $S^u$  and backward cone conditions for  $Q_s$  in  $S^u$ .
2. Every forward trajectory starting from a point in the sector  $S^u$  must exit the sector.
3. The flow  $\Phi_t$  is backward outflowing from  $S^u$  along  $Q_s$ .

Then the unstable manifold  $W^u(\tilde{\Lambda})$  is contained in  $S^u$ . Moreover,  $w^u$  is Lipschitz, with Lipschitz constant  $L_{cu}$ . (The  $L_{cu}$  is the constant in the cone  $Q_{cu}$ ; see (8)).

**Theorem 17.** Let  $S^s$  be a sector (see Definition 6) and denote by  $\Phi_t$  the flow induced by  $F$ . Assume that:

1. The flow  $\Phi_t$  satisfies backward cone conditions for  $Q_{cs}$  in  $S^s$  and forward cone conditions for  $Q_u$  in  $S^s$ .
2. Every backward trajectory starting from a point in the sector  $S^s$  must exit the sector.

3. The flow  $\Phi_t$  is forward outflowing from  $S^s$  along  $Q_u$ .

Then the stable manifold  $W^s(\tilde{\Lambda})$  is contained in  $S^s$ . Moreover,  $w^s$  is Lipschitz, with the Lipschitz constant  $L_{cs}$ . (The  $L_{cs}$  is the constant in the cone  $Q_{cu}$ ; see (8).)

We will focus on proving Theorem 16, since Theorem 17 follows from Theorem 16 by reversing the sign of the vector field and swapping the roles of the coordinates  $x$  and  $y$ .

Before we prove Theorem 16, we need some additional notions and technical lemmas. To simplify the notation, throughout this section let us write here

$$x = (x, \lambda).$$

**Definition 18.** We say that  $h : \pi_x \overline{S^u} \rightarrow \overline{S^u}$  is a center-horizontal disc satisfying  $Q_{cu}$  cone condition if

$$\pi_x h = \text{Id}_x, \quad (9)$$

and for every  $x_1, x_2 \in \pi_x \overline{S^u}$ , such that  $h(x_1), h(x_2)$  lie in a single chart,

$$Q_{cu}(h(x_1) - h(x_2)) \geq 0. \quad (10)$$

For discs  $h$  as defined above we will write

$$\text{graph}(h) := h(\pi_x \overline{S^u}).$$

**Remark 19.** In our proof of Theorem 16 we will show that there exists a center-horizontal disc  $w^u$  satisfying  $Q_{cu}$  cone condition such that

$$W^u(\tilde{\Lambda}) = \text{graph}(w^u).$$

The lemma below will be the main building block for the construction of  $W^u(\tilde{\Lambda})$  in the proof of Theorem 16.

**Lemma 20.** Assume that  $S^u$  is an unstable sector and  $\Phi_t$  satisfies forward cone conditions for  $Q_{cu}$ , then there exists  $T > 0$  such that for every center-horizontal disc satisfying  $Q_{cu}$  cone condition  $h : \pi_x S^u \rightarrow S^u$  there exists a center-horizontal disc satisfying  $Q_{cu}$  cone conditions  $h' : \pi_x S^u \rightarrow S^u$  such that

$$\Phi_T(\text{graph}(h)) \cap S^u = \text{graph}(h').$$

Moreover, if for  $q \in \text{graph}(h)$  we have  $\Phi_T(q) \in S^u$ , then  $q \in \text{graph}(h')$  and  $\Phi_t(q) \in S^u$  for  $t \in [0, T]$ .

**Proof.** Let  $r \in (0, \pi)$  be fixed. By the continuity of the flow with respect to time and initial conditions, for every  $q_1 \in \overline{S^u}$  there exists a  $T > 0$  such that for all  $t \in [0, T]$  and all  $q_2$  such that  $\|q_1 - q_2\| = r$  we have

$$\frac{r}{2} < \|\Phi_t(q_2) - q_1\| < \pi. \quad (11)$$

By compactness of  $\overline{S^u}$  the  $T$  can be chosen to be independent of the choice of  $q_1$ . Since the points in  $S^u_-$  exit the set  $S^u$  (see Condition 1 from Definition 5), and  $S^u_-$  is compact, we can choose  $T$  small enough so that in addition to (11),

$$\Phi_t(q) \notin S^u, \quad \text{for every } t \in [0, 2T] \text{ and } q \in S^u_-. \quad (12)$$

Condition (12) ensures that if we exit the set  $S^u$  then we can not return to it in a time shorter than  $2T$ . This implies that if  $q \in S^u$  and  $\Phi_T(q) \in S^u$ , then  $\Phi_t(q) \in S^u$  for all  $t \in [0, T]$ .

Let us introduce the following notation. We will write  $\mathbf{x} = (x, \lambda)$  for a point in  $\mathbb{R}^u \times \Lambda$ . Let us also introduce the following set

$$\mathcal{D}_u := \pi_{\mathbf{x}} S^u$$

Observe that  $\partial \mathcal{D}_u := \pi_{\mathbf{x}} \partial S^u = \pi_{\mathbf{x}} S^u_-$ .

For a given center-horizontal disc  $h$  satisfying the  $Q_{cu}$  cone condition and fixed  $t \in \mathbb{R}$ , let us define  $g_t : \overline{\mathcal{D}_u} \rightarrow \mathbb{R}^u \times \Lambda$

$$g_t(\mathbf{x}) = \pi_{\mathbf{x}} \Phi_t \circ h(\mathbf{x}).$$

(The function  $g_t$  depends on the choice of  $h$ .) For small  $t$  the function  $g_t$  is close to identity. From (11–12), for every  $t \in [0, T]$ ,

$$\frac{r}{2} < \|g_t(\mathbf{x}_2) - \mathbf{x}_1\| < \pi \quad \text{for all } \mathbf{x}_1 \in \overline{\mathcal{D}_u} \text{ and } \mathbf{x}_2 \in \partial B(\mathbf{x}_1, r) \cap \overline{\mathcal{D}_u}, \quad (13)$$

$$g_t(\mathbf{x}_3) \notin \mathcal{D}_u \quad \text{for all } \mathbf{x}_3 \in \partial \mathcal{D}_u. \quad (14)$$

Note that the choice of  $T$  is independent from  $h$ .

We will show that for every  $\mathbf{x}_1 \in \mathcal{D}_u$  there exists a point  $\mathbf{x}'_1 \in \mathcal{D}_u$  such that  $g_T(\mathbf{x}'_1) = \mathbf{x}_1$ . We will prove this by using the local Brouwer degree (see Appendix). To do so, we will construct a homotopy from  $g_T$  to the identity map with some good properties. Let  $U = B(\mathbf{x}_1, r) \cap \mathcal{D}_u$ . Let  $H : [0, 1] \times U \rightarrow \mathbb{R}^{u+c}$  be a homotopy chosen as

$$H(\alpha, \mathbf{x}) = g_{\alpha T}(\mathbf{x}).$$

Note that

$$H(0, \mathbf{x}) = \mathbf{x}, \quad H(1, \mathbf{x}) = g_T(\mathbf{x}).$$

From (13–14) we see that for  $\mathbf{x}_2 \in \partial B(\mathbf{x}_1, r) \cap \overline{\mathcal{D}_u}$  and  $\mathbf{x}_3 \in \partial \mathcal{D}_{cu}$

$$H(\alpha, \mathbf{x}_i) \neq \mathbf{x}_1, \quad \text{for } i = 2, 3. \quad (15)$$

Since  $\partial U = (\partial B(\mathbf{x}_1, r) \cap \overline{\mathcal{D}_u}) \cup (\overline{B(\mathbf{x}_1, r)} \cap \partial \mathcal{D}_u)$ , (15) implies that for every  $\mathbf{x} \in \partial U$  and every  $\alpha \in [0, 1]$

$$\mathbf{x}_1 \notin H([0, 1], \partial U).$$

By the homotopy property of the Brouwer degree

$$\begin{aligned} \deg(g_T, U, \mathbf{x}_1) &= \deg(H(1, \cdot), U, \mathbf{x}_1) = \deg(H(0, \cdot), U, \mathbf{x}_1) \\ &= \deg(\text{Id}, U, \mathbf{x}_1) = 1, \end{aligned}$$

hence by the solution property of the Brouwer degree we see that there exists an  $\mathbf{x}'_1 \in U \subset \mathcal{D}_u$  such that

$$g_T(\mathbf{x}'_1) = \mathbf{x}_1.$$

Above we have shown that  $\mathcal{D}_u \subset g_T(\mathcal{D}_{cu})$ , hence from the continuity of  $g_T$  and compactness of  $\overline{\mathcal{D}_u}$ ,  $g_T(\overline{\mathcal{D}_u})$  is compact and  $\overline{\mathcal{D}_u} \subset g_T(\overline{\mathcal{D}_{cu}})$ .

Now we will show that  $g_T : \overline{\mathcal{D}_u} \rightarrow \mathbb{R}^u \times \Lambda$  is injective. By choosing small  $T$  the map  $g_T$  is close to identity. It is therefore enough to show that for  $x_1 \neq x_2$  close enough so that  $h(x_1) - h(x_2)$  are in the same chart, we will have  $g_T(x_1) \neq g_T(x_2)$ . For  $x_1 \neq x_2$  we know that

$$Q_{cu}(h(x_1) - h(x_2)) \geq 0,$$

so, by the fact that  $\Phi_t$  satisfies cone conditions for  $Q_{cu}$  we also have

$$0 \leq Q_{cu}(\Phi_T(h(x_1)) - \Phi_T(h(x_2))),$$

which implies

$$\begin{aligned} \|\pi_y[\Phi_T(h(x_1)) - \Phi_T(h(x_2))]\| &\leq L_{cu} \|\pi_x[\Phi_T(h(x_1)) - \Phi_T(h(x_2))]\| \\ &= L_{cu} \|g_T(x_1) - g_T(x_2)\|. \end{aligned} \quad (16)$$

If  $\pi_y[\Phi_T(h(x_1)) - \Phi_T(h(x_2))] \neq 0$ , then above implies that  $g_T(x_1) \neq g_T(x_2)$ . If  $\pi_y[\Phi_T(h(x_1)) - \Phi_T(h(x_2))] = 0$  then we see that since by uniqueness of solutions of ODEs  $\Phi_T(h(x_1)) \neq \Phi_T(h(x_2))$  we must also have  $g_T(x_1) \neq g_T(x_2)$ .

Above argument shows that also  $g_t$  is injective, for every  $t \in [0, T]$ .

Let us now define

$$h'(x) := \Phi_T(h(g_T^{-1}(x))). \quad (17)$$

By definition of  $h'$  we see that  $\pi_x h'(x) = \pi_x \Phi_T(h(g_T^{-1}(x))) = g_T(g_T^{-1}(x)) = x$ . From (16) we see that

$$\begin{aligned} \|\pi_y[h'(x_1) - h'(x_2)]\| &= \|\pi_y[\Phi_T(h(g_T^{-1}(x_1))) - \Phi_T(h(g_T^{-1}(x_2)))]\| \\ &\leq L_{cu} \|\pi_x[\Phi_T(h(g_T^{-1}(x_1))) - \Phi_T(h(g_T^{-1}(x_2)))]\| \\ &= L_{cu} \|x_1 - x_2\|. \end{aligned}$$

Hence  $Q_{cu}(h'(x_1) - h'(x_2)) \geq 0$ , so  $h'$  so satisfies  $Q_{cu}$  cone condition.

What remains is to show that  $\text{graph}(h') \subset \overline{S^u}$ . Points can exit  $\overline{S^u}$  along a forward trajectory only through the set  $S_-^u$ . Once they exit, due to our choice of  $T$  they can not come back to  $\overline{S^u}$ . Moreover,  $g_T(x)$  is injective. This means that  $h'$  contains only points  $\Phi_T \circ h(x)$  for which  $\Phi_{[0, T]} \circ h(x) \subset \overline{S^u}$ , hence  $h' \subset \overline{S^u}$ . As required. ■

We are now ready to prove Theorem 16.

**Proof of Theorem 16.** Let  $T$  be as obtained in Lemma 20.

For a given center-horizontal disc  $h$  satisfying  $Q_{cu}$  cone conditions, by Lemma 20 we know that there exists the disc  $h'$ . Let us introduce the notation  $\mathcal{G}(h) := h'$ .

We shall now construct  $w^u$ . The idea is to take  $h_0(x) = (\pi_x x, 0, \pi_\lambda x)$ , inductively define  $h_{n+1} := \mathcal{G}(h_n)$  for  $n \geq 0$ , and show that  $h_{n+1}$  converges to  $w^u$ .

Consider  $h_n$  as defined above. Let  $x \in \pi_x S^u$  be fixed. By compactness of  $\{p \in \overline{S^u} : \pi_x p = x\}$  and the fact that  $\pi_x h_n(x) = x$ , there exists a convergent subsequence  $\lim_{k \rightarrow \infty} h_{n_k}(x) = q$ . We will show that such  $q$  has to be unique. Suppose that for two subsequences  $m_k$  and  $n_k$  we have  $\lim_{k \rightarrow \infty} h_{m_k}(x) = q_1$  and  $\lim_{k \rightarrow \infty} h_{n_k}(x) = q_2$ .

Let us fix  $t > 0$ . We have  $\Phi_{-t}(q_1) = \lim_{k \rightarrow \infty} \Phi_{-t}(h_{m_k}(x))$  and  $\Phi_{-t}(h_{m_k}(x)) \in S^u$  for  $m_k$  large enough ( $t < m_k \cdot T$ ). Hence  $\Phi_{-t}(q_1) \in S^u$ . For  $q_2$ , by analogous argument, we also obtain  $\Phi_{-t}(q_2) \in S^u$ .

Since  $\pi_x q_1 = x = \pi_x q_2$ , we see that  $Q_s(q_1 - q_2) \geq 0$ , and since the  $\Phi_{-t}$  is outflowing along  $Q_s$  we see that  $q_1$  has to be equal to  $q_2$ , otherwise one of them would exit  $S^u$ .

We now define  $w^u(x) = \lim_{n \rightarrow \infty} h_n(x)$ . The conditions (9–10) are preserved by passing to the limit, which concludes the construction of  $w^u$ . In particular, the graph of  $w^u$  is  $L_{cu}$ -Lipschitz.

By construction, the center horizontal disc graph ( $w^u$ ) consists of points, whose backward trajectories remain in  $S^u$ .

By repeating the above argument leading to  $q_1 = q_2$  we can easily prove that any point whose backward trajectory remains in  $S^u$  has to be in  $\text{graph}(w^u)$ . Moreover, since the forward trajectory starting from every point from  $S^u$  must exit the sector, a backward trajectory which remains in  $S^u$  must accumulate on a limit set contained in the boundary  $\partial S^u$ . Note that  $\partial S^u = S_-^u \cup S_+^u \cup \tilde{\Lambda}$ . All points from  $S_-^u$  exit  $\overline{S^u}$  and all points from  $S_+^u$  enter  $S^u$ . This means that any backward trajectory which remains in  $S^u$  must converge to  $\tilde{\Lambda}$ .

This concludes the proof. ■

### 3.3. Validation of cone and outflowing conditions based on contraction/expansion rates

In this section we introduce ‘rates’ of contraction and expansion associated to a matrix and show how they can be used to validate cone conditions and outflowing conditions. The conditions follow from estimates on the matrices  $G$  appearing in (6). The tools presented in this section make the abstract Theorems 16 and 17 a practical tool for establishing the existence of the invariant manifolds.

Once again, we focus on the case of the unstable manifold, since the stable manifold follows from changing the sign of the vector field and swapping the roles of the coordinates  $x, y$ .

Throughout this section we keep the notation

$$x = (x, \lambda).$$

Assume that (6) is satisfied, i.e. that

$$DF(x, y) = h(x, y)G(x, y), \quad \text{for } (x, y) \in S^u,$$

where

$$h(x, y) > 0 \quad \text{for } (x, y) \in S^u. \quad (18)$$

Consider the matrix  $G$  of the form

$$G(p) = \begin{pmatrix} G_{xx}(p) & G_{xy}(p) \\ G_{yx}(p) & G_{yy}(p) \end{pmatrix} \quad \text{for } p \in \overline{S^u},$$

where  $G_{xx}$ ,  $G_{xy}$ ,  $G_{yx}$  and  $G_{yy}$  are  $(c+u) \times (c+u)$ ,  $(c+u) \times s$ ,  $s \times (c+u)$  and  $s \times s$  matrices, respectively. Let us define the following constants (see (3)),

$$\begin{aligned} m_l(G_{xx}) &:= \inf_{p \in \overline{S^u}} m_l(G_{xx}(p)), & l(G_{yy}) &:= \sup_{p \in \overline{S^u}} l(G_{yy}(p)), \\ \|G_{xy}\| &:= \sup_{p \in \overline{S^u}} \|G_{xy}(p)\|, & \|G_{yx}\| &:= \sup_{p \in \overline{S^u}} \|G_{yx}(p)\|. \end{aligned}$$

**Definition 21.** Let  $\xi_{cu}, \mu_s \in \mathbb{R}$  be defined as

$$\begin{aligned} \xi_{cu} &:= m_l(G_{xx}) - L_{cu} \|G_{xy}\|, \\ \mu_s &:= l(G_{yy}) + \frac{1}{L_{cu}} \|G_{yx}\|. \end{aligned} \quad (19)$$

We refer to  $\xi_{cu}$  as the expansion rate of  $G$  and to  $\mu_s$  as the contraction rate of  $G$ .

The lemma below provides a tool for validating cone conditions based on the expansion and contraction rates.

**Lemma 22.** *If the constants  $\xi_{cu}, \mu_s$  defined by (19) have the property*

$$\mu_s < \xi_{cu}, \quad (20)$$

*then the flow induced by (4) satisfies  $Q_{cu}$  cone conditions in  $S^u$ .*

**Proof.** By Lemma 8 from [24] we know that  $m(I + tA) = 1 + tm_l(A) + O(t^2)$  and the bound  $O(t^2)$  is uniform if we consider matrices  $A$  in some compact set. In our case this compact set is given as  $\{DF(p), p \in \overline{S^u}\}$ .

Let  $p_1 \neq p_2$ ,  $p_i = (x_i, y_i)$  for  $i = 1, 2$ , be such that  $Q_{cu}(p_1 - p_2) \geq 0$ . Since  $\|y_1 - y_2\| \leq L_{cu} \|x_1 - x_2\|$  and  $h \geq 0$ , by (3) and Lemma 4, for  $t > 0$

$$\begin{aligned} & \frac{1}{t} (\|\pi_x(\Phi_t(p_1) - \Phi_t(p_2))\| - \|x_1 - x_2\|) \\ &= \frac{1}{t} (\|(x_1 - x_2) + t\pi_x(F(p_1) - F(p_2)) + O(t^2)\| - \|x_1 - x_2\|) \\ &= \left\| \frac{1}{t} \left( \text{Id}_x + t \int_0^1 \pi_x \frac{\partial F}{\partial x}(p_1 + s(p_1 - p_2)) ds \right) (x_1 - x_2) \right. \\ & \quad \left. + \int_0^1 \pi_x \frac{\partial F}{\partial y}(p_1 + s(p_1 - p_2)) ds (y_1 - y_2) \right\| - \frac{1}{t} \|x_1 - x_2\| + O(t) \\ &\geq \frac{1}{t} \left( m \left( \text{Id}_x + t \int_0^1 \pi_x \frac{\partial F}{\partial x}(p_1 + s(p_1 - p_2)) ds \right) - 1 \right) \|x_1 - x_2\| \\ & \quad - \int_0^1 \left\| \pi_x \frac{\partial F}{\partial y}(p_1 + s(p_1 - p_2)) \right\| ds L_{cu} \|x_1 - x_2\| + O(t) \\ &= m_l \left( \int_0^1 \pi_x \frac{\partial F}{\partial x}(p_1 + s(p_1 - p_2)) ds \right) \|x_1 - x_2\| + O(t) \\ & \quad - L_{cu} \int_0^1 \left\| \pi_x \frac{\partial F}{\partial y}(p_1 + s(p_1 - p_2)) \right\| ds \|x_1 - x_2\| + O(t) \\ &= m_l \left( \int_0^1 (h \cdot G_{xx})(p_1 + s(p_1 - p_2)) ds \right) \|x_1 - x_2\| + O(t) \\ & \quad - L_{cu} \int_0^1 \|(h \cdot G_{xy})(p_1 + s(p_1 - p_2))\| ds \|x_1 - x_2\| + O(t) \\ &\geq (m_l(G_{xx}) - L_{cu} \|G_{xy}\|) \int_0^1 h(p_1 + s(p_1 - p_2)) ds \|x_1 - x_2\| + O(t) \\ &= \xi_{cu} \int_0^1 h(p_1 + s(p_1 - p_2)) ds \|x_1 - x_2\| + O(t). \end{aligned} \quad (21)$$

So, letting  $t \rightarrow 0$ ,

$$D_- \|\pi_x(\Phi_t(p_1) - \Phi_t(p_2))\|_{t=0} \geq \xi_{cu} \int_0^1 h(p_1 + s(p_1 - p_2)) ds \|x_1 - x_2\|, \quad (22)$$

where

$$D_- f(t_0) = \liminf_{t \rightarrow 0^+} \frac{f(t_0 + t) - f(t_0)}{t}$$

is the lower Dini derivative of  $f$ .

By Lemma 7 from [24], we know that  $\|I + tA\| = 1 + t\ell(A) + O(t^2)$  and the bound  $O(t^2)$  is uniform if we consider matrices  $A$  in some compact set. By using the fact that  $h \geq 0$  together with Lemma 3, for  $t > 0$ ,

$$\begin{aligned} & \frac{1}{t} (\|\pi_y(\Phi_t(p_1) - \Phi_t(p_2))\| - \|y_1 - y_2\|) \\ &= \frac{1}{t} (\|(y_1 - y_2) + t\pi_y(F(p_1) - F(p_2)) + O(t^2)\| - \|y_1 - y_2\|) \\ &= \left\| \frac{1}{t} \left( \text{Id}_y + t \int_0^1 \pi_y \frac{\partial F}{\partial y}(p_1 + s(p_1 - p_2)) ds \right) (y_1 - y_2) \right. \\ & \quad \left. + \int_0^1 \pi_y \frac{\partial F}{\partial x}(p_1 + s(p_1 - p_2)) ds (x_1 - x_2) \right\| - \frac{1}{t} \|y_1 - y_2\| + O(t) \\ &\leq \frac{1}{t} \left( \left\| \left( \text{Id}_y + t \int_0^1 \pi_y \frac{\partial F}{\partial y}(p_1 + s(p_1 - p_2)) ds \right) \right\| - 1 \right) L_{cu} \|x_1 - x_2\| \\ & \quad + \int_0^1 \left\| \pi_y \frac{\partial F}{\partial x}(p_1 + s(p_1 - p_2)) \right\| ds \|x_1 - x_2\| + O(t) \\ &= l \left( \int_0^1 \pi_y \frac{\partial F}{\partial y}(p_1 + s(p_1 - p_2)) ds \right) L_{cu} \|x_1 - x_2\| + O(t) \\ & \quad + \int_0^1 \left\| \pi_y \frac{\partial F}{\partial x}(p_1 + s(p_1 - p_2)) \right\| ds \|x_1 - x_2\| + O(t) \\ &\leq L_{cu} \left[ l(G_{yy}) + \frac{1}{L_{cu}} \|G_{yx}\| \right] \|x_1 - x_2\| \int_0^1 h(p_1 + s(p_1 - p_2)) ds + O(t) \\ &= L_{cu} \mu_s \int_0^1 h(p_1 + s(p_1 - p_2)) ds \|x_1 - x_2\| + O(t). \end{aligned}$$

So, letting  $t \rightarrow 0$ ,

$$D^+ \|\pi_y(\Phi_t(p_1) - \Phi_t(p_2))\|_{|t=0} \leq L_{cu} \mu_s \int_0^1 h(p_1 + s(p_1 - p_2)) ds \|x_1 - x_2\|, \quad (23)$$

where

$$D_+ f(t_0) = \limsup_{t \rightarrow 0^+} \frac{f(t_0 + t) - f(t_0)}{t}$$

is the upper Dini derivative of  $f$ .

These estimates of the Dini derivatives imply

$$D_- (L_{cu} \|x_1(t) - x_2(t)\| - \|y_1(t) - y_2(t)\|)_{|t=0} > 0. \quad (24)$$

Indeed, using (18), (20), (22), (23) we obtain

$$\begin{aligned}
& D_- (L_{cu} \|x_1(t) - x_2(t)\| - \|y_1(t) - y_2(t)\|) |_{t=0} \\
& \geq L_{cu} D_- \|\pi_x(\Phi_t(p_1) - \Phi_t(p_2))\| |_{t=0} - D^+ \|\pi_y(\Phi_t(p_1) - \Phi_t(p_2))\| |_{t=0} \\
& \geq L_{cu} \xi_{cu} \int_0^1 h(p_1 + s(p_1 - p_2)) ds \|x_1 - x_2\| \\
& \quad - L_{cu} \mu_s \int_0^1 h(p_1 + s(p_1 - p_2)) ds \|x_1 - x_2\| \\
& = (\xi_{cu} - \mu_s) L_{cu} \int_0^1 h(p_1 + s(p_1 - p_2)) ds \|x_1 - x_2\| \\
& > 0.
\end{aligned}$$

Finally, if we assume that  $L_{cu} \|x_1 - x_2\| - \|y_1 - y_2\| \geq 0$  (i.e. we are also possibly on the boundary of the cone), the inequality (24) implies  $Q_{cu}$  forward cone conditions. We have thus proven that the flow satisfies  $Q_{cu}$  cone conditions on  $S^u$ . ■

We now discuss how to validate backward  $Q_s$  cone condition (see Definition 13) and outflowing from  $S^u$  condition (see Definition 15). To this end, we define the following two constants

$$\begin{aligned}
\xi_s & := m_l(-G_{yy}) - L_s \|G_{yx}\|, \\
\mu_{cu} & := l(-G_{xx}) + \frac{1}{L_s} \|G_{xy}\|.
\end{aligned}$$

**Lemma 23.** *If*

$$\mu_{cu} < \xi_s \quad \text{and} \quad \xi_s > 0,$$

*then we have backward cone condition for  $Q_s$  in  $S^u$  and the backward outflowing condition from  $S^u$  along  $Q_s$ .*

**Proof.** If we reverse the sign in the vector field (which then induces the flow with reversed time), then  $\xi_s$  plays the role of an expansion rate, and  $\mu_{cu}$  the role of the contraction rate. This means that from Lemma 22 we obtain backward cone conditions for  $Q_s$  in  $S^u$ .

We now turn to proving the outflowing from  $S^u$  along  $Q_s$  condition. From a mirror derivation to (21) for  $p_1 = (x_1, y_1)$  and  $p_2 = (x_2, y_2)$  such that  $\|x_1 - x_2\| \leq L_s \|y_1 - y_2\|$

and for  $t > 0$  we obtain

$$\begin{aligned}
& \frac{1}{t} (\|\pi_y(\Phi_{-t}(p_1) - \Phi_{-t}(p_2))\| - \|y_1 - y_2\|) \\
&= \frac{1}{t} (\|(y_1 - y_2) + t\pi_y(-F(p_1) + F(p_2)) + O(t^2)\| - \|y_1 - y_2\|) \\
&= \left\| \frac{1}{t} \left( \text{Id}_y + t \int_0^1 \pi_y \frac{-\partial F}{\partial y}(p_1 + s(p_1 - p_2)) ds \right) (y_1 - y_2) \right. \\
&\quad \left. + \int_0^1 \pi_y \frac{-\partial F}{\partial x}(p_1 + s(p_1 - p_2)) ds (x_1 - x_2) \right\| - \frac{1}{t} \|y_1 - y_2\| + O(t) \\
&\geq \frac{1}{t} \left( m \left( \text{Id}_y + t \int_0^1 \pi_y \frac{-\partial F}{\partial y}(p_1 + s(p_1 - p_2)) ds \right) - 1 \right) \|y_1 - y_2\| \\
&\quad - \int_0^1 \left\| \pi_y \frac{-\partial F}{\partial x}(p_1 + s(p_1 - p_2)) \right\| ds L_s \|y_1 - y_2\| + O(t) \\
&= m_l \left( \int_0^1 \pi_y \frac{-\partial F}{\partial y}(p_1 + s(p_1 - p_2)) ds \right) \|y_1 - y_2\| + O(t) \\
&\quad - L_s \int_0^1 \left\| \pi_y \frac{-\partial F}{\partial x}(p_1 + s(p_1 - p_2)) \right\| ds \|y_1 - y_2\| + O(t) \\
&\geq (m_l(-G_{yy}) - L_s \|G_{yx}\|) \int_0^1 h(p_1 + s(p_1 - p_2)) ds \|y_1 - y_2\| + O(t) \\
&= \xi_s \int_0^1 h(p_1 + s(p_1 - p_2)) ds \|y_1 - y_2\| + O(t).
\end{aligned}$$

Now, since for  $p \in S^u$  we have  $h(p) > 0$  and  $\xi_s > 0$ , for sufficiently small  $t > 0$  we obtain

$$\|\pi_y(\Phi_{-t}(p_1) - \Phi_{-t}(p_2))\| > \|y_1 - y_2\|. \quad (25)$$

Recall that we are assuming that  $p_1 \neq p_2$  satisfy  $Q_s(p_1 - p_2) \geq 0$ . Up to now, we have proven that, for  $t > 0$  and as long as  $\Phi_{-t}(p_1), \Phi_{-t}(p_2) \in S^u$ , the following is satisfied:

- Since  $Q_s^+(p) \cap S^u$  is in a single chart, for every  $p \in S^u$  and  $t > 0$ ,

$$Q_s(\Phi_{-t}(p_1) - \Phi_{-t}(p_2)) \geq 0.$$

- The map  $t \rightarrow \|\pi_y(\Phi_{-t}(p_1) - \Phi_{-t}(p_2))\|$  is strictly increasing.

We will show that this implies that for some  $t > 0$  either  $\Phi_{-t}(p_1)$  or  $\Phi_{-t}(p_2)$  must exit  $S^u$ .

If this was not the case, by compactness of  $\overline{S^u}$  we would have a sequence  $t_n \rightarrow \infty$  and a point  $p_1^* = \lim_{n \rightarrow \infty} \Phi_{-t_n}(p_1)$ . From compactness, we can choose a subsequence  $t_{n_k}$  such that  $p_2^* = \lim_{k \rightarrow \infty} \Phi_{-t_{n_k}}(p_2)$ . Since by the  $Q_s$ -backward cone condition  $\Phi_{-t_{n_k}}(p_1) \in Q_s^+(\Phi_{-t_{n_k}}(p_2))$ , by passing to the limit, we obtain  $p_1^* \in Q_s^+(p_2^*)$ . Also

$$\left\| \pi_y \left( \Phi_{-t_{n_k}}(p_1) - \Phi_{-t_{n_k}}(p_2) \right) \right\| \xrightarrow{k \rightarrow \infty} \|\pi_y(p_1^* - p_2^*)\|,$$

and by the strict monotonicity of  $t \mapsto \|\pi_y(\Phi_{-t}(p_1) - \Phi_{-t}(p_2))\|$

$$\|\pi_y(\Phi_{-t}(p_1) - \Phi_{-t}(p_2))\| < \|\pi_y(p_1^* - p_2^*)\|, \quad \text{for all } t > 0. \quad (26)$$

Observe that from the above condition it follows that  $\pi_y p_1^* \neq \pi_y p_2^*$ . Hence at least one of the points  $p_1^*, p_2^*$  must not belong to  $\Lambda$ , so that (25) holds and the function  $t \mapsto \|\pi_y(\Phi_{-t}(p_1^*) - \Phi_{-t}(p_2^*))\|$  is increasing.

Taking any  $s > 0$ . We have,

$$\|\pi_y(p_1^* - p_2^*)\| > \left\| \pi_y \left( \Phi_{-t_{n_k} - s}(p_1) - \Phi_{-t_{n_k} - s}(p_2) \right) \right\|.$$

Taking the limit  $k \rightarrow \infty$ , we obtain a contradiction:

$$\|\pi_y(p_1^* - p_2^*)\| > \|\pi_y(\Phi_{-s}(p_1^*) - \Phi_{-s}(p_2^*))\| > \|\pi_y(p_1^* - p_2^*)\|.$$

This finishes our proof. ■

#### 4. Description of the PCR3BP at infinity

In this section we introduce the Planar Circular Restricted 3-Body Problem and present several sets of coordinates that will be useful in our construction.

##### 4.1. Equations at infinity

Let  $(r, \alpha)$  be polar coordinates in the plane and let  $(y, G)$  be their symplectic conjugate momenta, i.e.  $y = \dot{r}$  is the momentum in the radial direction and  $G = r^2 \dot{\alpha}$  is the angular momentum. Then, the Hamiltonian for the planar circular restricted three body problem (PCR3BP) in the inertial frame, where the primaries are rotating, takes the form

$$\mathcal{H}(r, \alpha, y, G, t) = \frac{1}{2} \left( \frac{G^2}{r^2} + y^2 \right) - U(r, \alpha - t), \quad (27)$$

where

$$U(r, \phi) = \frac{1 - \mu}{\sqrt{r^2 + 2\mu r \cos \phi + \mu^2}} + \frac{\mu}{\sqrt{r^2 - 2(1 - \mu)r \cos \phi + (1 - \mu)^2}}$$

is the Newtonian potential describing the interaction of the massless body with the primaries, which move on circular orbits. In the rotating coordinate frame  $\phi = \alpha - t$ , the Hamiltonian (27) becomes the Hamiltonian  $H$  in (1) in polar coordinates, that is

$$H(r, \phi, y, G) = \frac{1}{2} \left( \frac{G^2}{r^2} + y^2 \right) - U(r, \phi) - G. \quad (28)$$

Since we want to study the invariant manifolds of infinity, we consider the McGehee coordinates  $(x, y, \phi, G)$  where

$$r = \frac{2}{x^2}, \quad x > 0. \quad (29)$$

Taking

$$\mathcal{U}(x, \phi) = U(2x^{-2}, \phi), \quad (30)$$

we obtain the following ODE

$$\begin{aligned} \dot{x} &= -\frac{1}{4}x^3y, \\ \dot{y} &= \frac{1}{8}x^6G^2 - \frac{x^3}{4}\frac{\partial\mathcal{U}}{\partial x}, \\ \dot{\phi} &= \frac{1}{4}x^4G - 1, \\ \dot{G} &= \frac{\partial\mathcal{U}}{\partial\phi}, \end{aligned} \quad (31)$$

which is reversible with respect to the involution

$$\mathcal{S}(x, y, \phi, G) = (x, -y, -\phi, G). \quad (32)$$

That is, the flow  $\Phi_t$  induced by (31) satisfies

$$\Phi_t \circ \mathcal{S} = \mathcal{S} \circ \Phi_{-t}. \quad (33)$$

Let us use the following notation  $\mathcal{O}_k(x) = \mathcal{O}(|x|^k)$ . Since  $(1+x)^{-1/2} = 1 - \frac{1}{2}x + \frac{3}{8}x^2 + \mathcal{O}_3(x)$ , one has

$$\begin{aligned} U(r, \phi) &= \frac{1-\mu}{r} \left( 1 + 2\frac{\mu}{r} \cos\phi + \left(\frac{\mu}{r}\right)^2 \right)^{-1/2} \\ &\quad + \frac{\mu}{r} \left( 1 - 2\frac{(1-\mu)}{r} \cos\phi + \left(\frac{1-\mu}{r}\right)^2 \right)^{-1/2} \\ &= \frac{1}{r} \left( 1 - \frac{\mu(1-\mu)}{2} (1 - 3\cos^2\phi) \frac{1}{r^2} + \mathcal{O}_1\left(\frac{\mu(1-\mu)}{r^3}\right) \right). \end{aligned}$$

Hence

$$\mathcal{U}(x, \phi) = U(2/x^2, \phi) = \frac{x^2}{2} \left( 1 - \frac{\mu(1-\mu)}{2} (1 - 3\cos^2\phi) \frac{x^4}{4} + \mathcal{O}(\mu x^6) \right). \quad (34)$$

Therefore,

$$\frac{\partial\mathcal{U}}{\partial x} = x + \mathcal{O}_5(x), \quad \frac{\partial\mathcal{U}}{\partial\phi} = \beta(\phi)x^6 + \mathcal{O}_8(x)$$

where

$$\beta(\phi) = \frac{3\mu(1-\mu)}{8} \cos\phi \sin\phi.$$

This means that in (31) in the equation for  $\dot{y}$  the dominant term near  $x = y = 0$  will be  $-\frac{x^3}{4}\frac{\partial\mathcal{U}}{\partial x} = -\frac{x^4}{4} + \mathcal{O}_6(x)$ .

The manifold at infinity

$$\Lambda = \{(x, y, \phi, G) \in \mathbb{R} \times \mathbb{R} \times \mathbb{T} \times \mathbb{R} \mid x = y = 0\},$$

is invariant and is foliated by periodic orbits

$$\Lambda_I = \Lambda \cap \{G = -I\}. \quad (35)$$

Observe that  $H \equiv 0$  on  $\Lambda$ .

**Remark 24.** In the definition of  $\Lambda_I$  we introduce the minus on the right hand side because then the periodic orbit  $\Lambda_I$  will belong to the energy level  $H = I$  (see (28)).

#### 4.2. Invariant sector

The system (31) can be written as

$$\begin{aligned} \dot{x} &= -\frac{1}{4}x^3y \\ \dot{y} &= -\frac{1}{4}x^4 + x^6\mathcal{O}_1 \\ \dot{\phi} &= \frac{1}{4}x^4G - 1 \\ \dot{G} &= \beta(\phi)x^6 + x^8\mathcal{O}_1, \end{aligned} \quad (36)$$

where  $\beta$  and all  $\mathcal{O}_1$  functions above are  $2\pi$ -periodic in  $\phi$ .

To straighten the lowest order terms, we make the change

$$\begin{aligned} q &= \frac{1}{2}(x - y), \\ p &= \frac{1}{2}(x + y), \\ \theta &= \phi + Gy. \end{aligned} \quad (37)$$

The coordinate change  $\theta = \phi + Gy$ , might appear artificial, as we are adding  $Gy$  to an angle  $\theta$ , however the system is still  $2\pi$ -periodic in  $\theta$ , which means that we can treat this variable as an angle.

Note that we are only interested in the region  $p + q \geq 0$  (see (29)). We do assume this fact throughout this section without mentioning it.

Then we have the new system, which has the form

$$\begin{aligned} \dot{q} &= \frac{1}{4}(q + p)^3 (q + (q + p)^3\mathcal{O}_0), \\ \dot{p} &= -\frac{1}{4}(q + p)^3 (p + (q + p)^3\mathcal{O}_0), \\ \dot{G} &= (p + q)^6\mathcal{O}_0, \\ \dot{\theta} &= (p + q)^6\mathcal{O}_0 - 1. \end{aligned} \quad (38)$$

Let  $F$  denote the vector field on the right hand side of (38). We note that the derivative of  $F$  is of the form

$$DF = (p + q)^3 \left( \frac{1}{4} \begin{pmatrix} 1 + \frac{3q}{q+p} & \frac{3q}{q+p} & 0 & 0 \\ -\frac{3p}{q+p} & -1 - \frac{3p}{q+p} & 0 & 0 \\ 0 & 0 & 0 & 0 \\ 0 & 0 & 0 & 0 \end{pmatrix} + \mathcal{O}_1 \right). \quad (39)$$

This means that we can factor out the term

$$h(q, p, \theta, G) = (p + q)^3,$$

in front of the derivative of the vector field.

On the level set of the Hamiltonian  $H = I$ , we have  $G = G(x, y, \theta, I)$ . From (28) we know that

$$I = \frac{x^4 G^2}{8} + \frac{1}{2} y^2 - \mathcal{U}(x, \phi) - G. \quad (40)$$

Since the equation (40) is quadratic in  $G$ , it can be explicitly solved for  $G(x, y, \theta, I)$ . The analytical formula has a singularity in the denominator for  $x \rightarrow 0$ , hence for the rigorous numerical computation of  $G$  and its derivatives it is convenient to use a different approach. Let us recall that by (34)  $\mathcal{U}(x, \phi) = x^2 \mathcal{O}_0$ , hence for  $x$  close to zero  $G$  can be solved for as  $G \approx -I$ .

Let  $I$  be fixed and let  $\varrho_I : \mathbb{R}^3 \times \mathbb{S}^1 \rightarrow \mathbb{R}$  be defined as

$$\varrho_I(q, p, G, \theta) := \frac{(p + q)^4 G^2}{8} + \frac{1}{2} (p - q)^2 - \mathcal{U}(p + q, \theta - G(p - q)) - G - I.$$

We consider  $G_I = G_I(q, p, \theta)$  to be the solution of  $\varrho_I(q, p, G_I, \theta) = 0$ , which satisfies  $G_I(0, 0, \theta) = -I$ . The lemma below is a tool which we use in our computer assisted proof to establish that such  $G_I$  is well defined and to validate explicit bounds for its values.

**Lemma 25.** *Let  $\mathbf{G}$  be a closed interval and let  $G_0 \in \text{int}\mathbf{G}$ . Let  $q, p, \theta$  be fixed. If*

$$G_0 - \left( \frac{\partial \varrho_I}{\partial G}(q, p, \mathbf{G}, \theta) \right)^{-1} \varrho_I(q, p, G_0, \theta) \subset \mathbf{G},$$

*then there exists a  $G_I(q, p, \theta) \in \mathbf{G}$  such that  $\varrho_I(q, p, G_I(q, p, \theta), \theta) = 0$ .*

**Proof.** The result follows from the interval Newton method [25, Theorem 13.2]. ■

**Corollary 26.** *Lemma 25 works under the implicit assumption that  $0 \notin \frac{\partial \varrho_I}{\partial G}(q, p, \mathbf{G}, \theta)$ , so from the implicit function theorem we also obtain that  $G_I(q, p, \theta) \in C^1$  and the bounds on its derivatives as*

$$\begin{aligned} \frac{\partial G_I}{\partial q}(q, p, \theta) &\in - \left( \frac{\partial \varrho_I}{\partial G}(q, p, \mathbf{G}, \theta) \right)^{-1} \frac{\partial \varrho_I}{\partial q}(q, p, \mathbf{G}, \theta), \\ \frac{\partial G_I}{\partial p}(q, p, \theta) &\in - \left( \frac{\partial \varrho_I}{\partial G}(q, p, \mathbf{G}, \theta) \right)^{-1} \frac{\partial \varrho_I}{\partial p}(q, p, \mathbf{G}, \theta), \\ \frac{\partial G_I}{\partial \theta}(q, p, \theta) &\in - \left( \frac{\partial \varrho_I}{\partial G}(q, p, \mathbf{G}, \theta) \right)^{-1} \frac{\partial \varrho_I}{\partial \theta}(q, p, \mathbf{G}, \theta). \end{aligned}$$

We see that in a neighborhood of  $\Lambda$  the coordinate  $q$  is “expanding”,  $p$  is “contracting”, and  $\theta, G$  are center coordinates. This means that we can expect the set

$$S^u = S_{I,L,R}^u := \{(q, p, G_I(q, p, \theta), \theta) : q \in (0, R), |p| < Lq, \theta \in \mathbb{S}^1\}, \quad (41)$$

to be an invariant sector (see Definition 5) for suitably chosen  $R, L > 0$ .

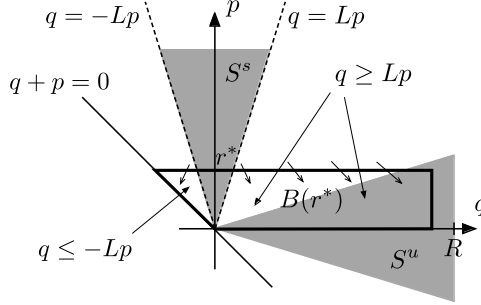


Figure 3: The set  $B(r^*)$  from Proposition 29.

**Remark 27.** We fix the energy level  $H = I$ , and for such fixed value our system becomes three dimensional. We therefore treat the sector  $S_{I,L,R}^u$  as a subset of a three dimensional space, with coordinates  $q, p, \theta$ .

The following lemma gives conditions to prove the existence of an unstable sector (according to Definition 5).

**Lemma 28.** Let  $F = (F_1, F_2, F_3, F_4) : \mathbb{R}^3 \times \mathbb{S}^1 \rightarrow \mathbb{R}^4$  stand for the vector field on the right hand side of (38). If for every

$$\begin{aligned} \langle (F_1, F_2)(z), (L, -1) \rangle &> 0 && \text{for all } z \in \{p = Lq\} \cap \overline{S_{I,L,R}^u}, \\ \langle (F_1, F_2)(z), (L, 1) \rangle &> 0 && \text{for all } z \in \{p = -Lq\} \cap \overline{S_{I,L,R}^u}, \\ F_1(z) &> 0 && \text{for all } z \in \{q = R\} \cap \overline{S_{I,L,R}^u}, \end{aligned}$$

then  $S_{I,L,R}^u$  is an unstable sector.

**Proof.** The assumptions imply that the flow can not exit  $S_{I,L,R}^u$  through  $|p| = Lq$  and must exit through  $\{q = R\}$ . ■

We define a sector

$$S^s = S_{I,L,R}^s := \{(q, p, G_I(q, p, \theta), \theta) : p \in (0, R), |q| < Lp, \theta \in \mathbb{S}^1\}. \quad (42)$$

The proposition below shows that points exiting a neighbourhood of  $\Lambda_I$  (within  $p+q > 0$ ) must do so through the unstable sector. This is a technical result, which will be useful in our construction for the proof of oscillatory motions in section 6.

**Proposition 29.** Assume that  $S^u$  and  $S^s$  defined in (41) and (42) are unstable invariant and stable sectors, respectively. Let

$$B(r) = \{(q, p, G_I(q, p, \theta), \theta) \mid -r < q < \sqrt{r}, 0 < p < r, \theta \in \mathbb{S}^1, q + p > 0\}.$$

There exists  $r^* > 0$ , such that:

1. For every

$$z_0 \in (B(r^*) \cap \{q > 0\}) \setminus (S^u \cup S^s)$$

there exists  $T = T(z_0) > 0$  such that  $z(T) \in S^u$ , where  $z(t)$  is a solution of (38) with initial condition  $z(0) = z_0$ .

2. For every

$$z_0 \in (B(r^*) \cap \{q < 0\}) \setminus S^s$$

and the solution  $z(t)$  starting from  $z_0$  we have

$$\lim_{t \rightarrow \infty} \pi_{q,p} z(t) = (q^*, p^*),$$

where  $p^* \in (-\pi_q z_0, r^*)$  and  $q^* + p^* = 0$ .

**Proof.** Below we will choose  $r^*$  sufficiently small so that  $r^* < 1$ ,  $\sqrt{r^*} < R$  and (see Figure 3)

$$(q = \sqrt{r^*}, p = r^*) \in \pi_{q,p} S^u = \pi_{q,p} S_{I,L,R}^u.$$

Observe that we have freedom to decrease  $r^*$  and still the above condition will be satisfied.

Let  $M$  be such that for  $\mathcal{O}_0$  in (38) we have a bound  $|\mathcal{O}_0| < M$  for some macroscopic neighborhood of  $(0, 0)$ . We choose  $r^*$  small enough so that  $B(r^*)$  lies in this neighbourhood.

We start by showing that if  $r^*$  is also small enough so that  $r^* < \frac{1}{64M^2}$  then for every point from  $\overline{B(r^*)} \cap \{p = r^*\}$  and any  $t$  holds

$$\frac{dp}{dt} < 0. \quad (43)$$

In view of (38) and the positivity of  $p + q$ , in order to show (43) it is enough to check that  $p + (p + q)^3 \mathcal{O}_0 > 0$ . Since  $|q| \leq \sqrt{r^*}$  and  $r^* < \frac{1}{64M^2}$  we obtain

$$p + (p + q)^3 \mathcal{O}_0 \geq r^* - M(r^* + \sqrt{r^*})^3 > r^* - M(2\sqrt{r^*})^3 > 0.$$

We can see from (43) that a trajectory can not exit the set  $B(r^*) \setminus (S^u \cup S^d)$  through  $\{p = r^*\}$ . (See Figure 3)

We now show that if we choose  $r^* < M^{-1} (1 + \frac{1}{L})^{-3}$  then for every point from  $(B(r^*) \cap \{q > 0\}) \setminus (S^u \cup S^s) \subset B(r^*) \cap \{q \geq Lp\}$  and any  $t$  holds

$$\frac{dq}{dt} > 0. \quad (44)$$

For this it is enough to show that  $q + (p + q)^3 \mathcal{O}_0 > 0$ . Since  $q \geq Lp$  and  $q \leq \sqrt{r^*} < \sqrt{M^{-1} (1 + \frac{1}{L})^{-3}}$  we see that

$$q + (p + q)^3 \mathcal{O}_0 \geq q - M(q + \frac{1}{L}q)^3 = q \left( 1 - q^2 M \left( 1 + \frac{1}{L} \right)^3 \right) > 0.$$

We are ready to prove the first claim. Let us fix  $z_0 \in (B(r^*) \cap \{q > 0\}) \setminus (S^u \cup S^s)$ . Let

$$c(z_0) = \min \left\{ \frac{dq}{dt}(z) : z = (q, p, G, \theta) \in B(r^*), \text{ such that } q \in [\pi_q z_0, \sqrt{r^*}], q \geq Lp \right\} > 0.$$

For a trajectory  $z(t)$  starting from  $z_0$ , for  $t > 0$  we will therefore have

$$\pi_q z(t) > \pi_q z_0 + c(z_0) t,$$

as long as  $z(t) \in B(r^*)$ . Since  $z(t)$  can not pass through  $\{p = r^*\}$  we will have  $z(T(z_0)) \in S^u$  for some  $T(z_0) < \sqrt{r^*}/c(z_0)$ .

To prove the second claim, observe that using mirror arguments to the proof of (44) we obtain that for every point from  $B(r^*) \cap \{q < 0\} \setminus S^s = B(r^*) \cap \{q \leq -Lp\}$  we have

$$\frac{dq}{dt} < 0.$$

For every point  $z_0 \in (B(r^*) \cap \{q < 0\}) \setminus S^s$  the trajectory  $z(t)$  which starts from  $z_0$  can not exit  $B(r^*)$  through  $\{p = r^*\}$ . Moreover it cannot exit through the line  $x = p + q = 0$  as it consist of the fixed points. Since  $q(t)$  is strictly increasing and bounded, it converges to  $q^* \in [-r^*, \pi_q z_0]$  and it is easy to see that then the trajectory must converge to the line  $x = p + q = 0$ . We have obtained

$$\lim_{t \rightarrow \infty} \pi_{q,p} z(t) = (q^*, p^*)$$

for some  $(q^*, p^*) \in \{q + p = 0\}$ . Therefore  $p^* = -q^* \in (-\pi_q z_0, r^*)$ . This finishes our proof. ■

#### 4.3. Bringing the factorised derivative at infinity to diagonal form

In the dominant part of matrix  $DF$  given by (39) in the limit of  $\frac{|p|}{q} \rightarrow 0$  (i.e. very tight sector) we have  $\frac{3q}{p+q} \rightarrow 3$  and  $\frac{3p}{p+q} \rightarrow 0$ . Therefore, we obtain there is an off-diagonal “non-small” term corresponding to the entry  $\frac{\partial F_q}{\partial p}$ . The presence of such term is undesirable, because it makes the verification of cone conditions for the parabolic invariant manifold harder.

In this section we discuss a simple change of coordinates of the form  $u = q + (1 - b)p$ , for some  $b \in \mathbb{R}$ , which leaves the remaining coordinates  $p, \theta, G$  unchanged. This change will take the derivative of the factorised vector field (39) at  $\Lambda$  to diagonal form.

By taking

$$u = q + (1 - b)p \tag{45}$$

we obtain the ODE

$$\begin{aligned} \dot{u} &= \frac{1}{4}(u + bp)^3 (u - 2(1 - b)p + (u + bp)^3 \mathcal{O}_0), \\ \dot{p} &= -\frac{1}{4}(u + bp)^3 (p + (u + bp)^3 \mathcal{O}_0), \\ \dot{G} &= (u + bp)^6 \mathcal{O}_0, \\ \dot{\theta} &= (u + bp)^6 \mathcal{O}_0 - 1. \end{aligned} \tag{46}$$

Let us denote the vector field on the right hand side in (46) by  $F = (F_u, F_p, F_G, F_\theta)$ .

It is easy to see that

$$\frac{\partial F_u}{\partial p} = \frac{1}{4}(u + bp)^3 (W + (u + bp)^2 \mathcal{O}_0),$$

where

$$\begin{aligned}
W &= \frac{3b}{u+bp} (u - 2(1-b)p) - 2(1-b) \\
&= 3b \frac{u}{u+bp} - 6b(1-b) \frac{p}{u+bp} - 2(1-b) \\
&= 3b \left( \frac{u}{u+bp} - 1 \right) - 6b(1-b) \frac{p}{u+bp} + (5b-2) \\
&= 3b \frac{-bp}{u+bp} - 6b(1-b) \frac{p}{u+bp} + (5b-2) \\
&= 3b(b-2) \frac{p}{u+bp} + (5b-2).
\end{aligned}$$

So if we take  $b = 2/5$ , then we get rid of the first term in the bracket and can factor out  $(u+bp)^3$  in front of the derivative of the vector field, obtaining

$$DF(u, p, G, \theta) = \frac{(u+bp)^3}{4} \left( \begin{pmatrix} 4 + 3(b-2) \frac{p}{u+bp} & 3b(b-2) \frac{p}{u+bp} & 0 & 0 \\ -3 \frac{p}{u+bp} & -1 - 3 \frac{p}{u+bp} & 0 & 0 \\ 0 & 0 & 0 & 0 \\ 0 & 0 & 0 & 0 \end{pmatrix} + \mathcal{O}_2(u+bp) \right). \quad (47)$$

with  $b = 2/5$ .

Since for points from a sector  $|p| \leq L_1 q$

$$\left| \frac{p}{u+bp} \right| = \left| \frac{p}{q+p} \right| \leq \frac{L_1}{1-L_1},$$

we see that for small  $L_1$  the factorised derivative of the vector field will be close  $\text{diag}(4, -1, 0, 0)$ , when computed at points from the sector.

## 5. Bounds on the unstable manifold at infinity in the PCR3BP

Let us fix  $I$  and consider the manifold  $\{H = I\}$  (see (28)) and the periodic orbit  $\Lambda_I$  introduced in (35). Analogously to (41), we consider a sector  $S_{I,L,R}^u$  in the coordinates  $(u, p, \theta)$ .

We will work in a setting where, by Lemma 25, for  $(u, p, G, \theta) \in \{J = I\}$ , we have  $G = G_I(u, p, \theta)$ . This means that  $(u, p, \theta)$  uniquely define the point  $(u, p, G_I(u, p, \theta), \theta)$ .

Our aim will be to apply Theorem 16 to establish the existence of a center-horizontal disc  $w^u : \overline{B}_u \times \mathbb{S}^1 \rightarrow S_{I,L,R}^u$ , for  $\overline{B}_u = [0, R] \subset \mathbb{R}$ , such that the unstable manifold  $W_{\Lambda_I}^u$  of  $\Lambda_I$  for the flow of (46) projected on to the  $u, p, \theta$  coordinates is a graph of  $w^u$

$$W_{\Lambda_I}^u = \text{graph}(w^u).$$

Recalling the change of coordinates (45) and that  $b = 2/5$ , we define

$$G_I(u, p, \theta) := G_I(u - (1-b)p, p, \theta).$$

From now on, for points belonging to the sector  $S_{I,L,R}^u$ , we denote by  $\tilde{\Phi}_t(u, p, \theta)$  the projection onto the  $(u, p, \theta)$  coordinates of the flow associated to (46) with initial condition at the point  $(u, p, G_I(u, p, \theta), \theta)$ .

Let  $P$  and  $M$  be the following matrices

$$P := \begin{pmatrix} 1 & 0 & 0 & 0 \\ 0 & 1 & 0 & 0 \\ 0 & 0 & 0 & 1 \end{pmatrix}, \quad M := \begin{pmatrix} 1 & 0 & 0 \\ 0 & 1 & 0 \\ \frac{\partial G_I}{\partial u} & \frac{\partial G_I}{\partial p} & \frac{\partial G_I}{\partial \theta} \\ 0 & 0 & 1 \end{pmatrix}.$$

On the invariant surface  $J = I$ , the coordinates are  $(u, p, \theta)$  and the vector field is  $\tilde{F}(u, p, \theta) = PF(u, p, G_I(u, p, \theta), \theta)$ . Hence the derivative of the vector field is

$$D\tilde{F}(u, p, \theta) := P DF(u, p, G_I(u, p, \theta), \theta) M. \quad (48)$$

From  $D\tilde{F}(u, p, \theta)$  we can factorise the term  $h(u, p, \theta) = (u + bp)^3$ . Let us use the notation  $\mathbf{G}$  for a  $3 \times 3$  interval matrix, which is an interval enclosure of the factorised  $D\tilde{F}$ . In other words, for every  $(u, p, \theta) \in \pi_{u,p,\theta} S_{I,L,R}^u$  let

$$D\tilde{F}(u, p, \theta) \in (u + bp)^3 \mathbf{G} = (u + bp)^3 \begin{pmatrix} \mathbf{G}_{uu} & \mathbf{G}_{up} & \mathbf{G}_{u\theta} \\ \mathbf{G}_{pu} & \mathbf{G}_{pp} & \mathbf{G}_{p\theta} \\ \mathbf{G}_{\theta u} & \mathbf{G}_{\theta p} & \mathbf{G}_{\theta\theta} \end{pmatrix}. \quad (49)$$

**Remark 30.** The  $\mathbf{G}$  can be obtained by validating assumptions of Lemma 25 to obtain bounds on  $G_I(u, p, \theta)$ , bounds on the derivatives of  $G_I$  via Corollary 26, and using these bounds for computing an interval enclosure of  $(u + bp)^{-3} P DF(z) M$  for all  $z \in S_{I,L,R}^u$ .

We now formulate our main result, which is our tool for obtaining the bounds on the unstable manifold of  $\Lambda_I$ . First we consider the following notation. As in (8) and (19), we define cones

$$\begin{aligned} Q_{cu}(u, p, \theta) &= L_{cu} \|(u, \theta)\| - \|p\|, \\ Q_s(u, p, \theta) &= L_s \|p\| - \|(u, \theta)\|, \end{aligned}$$

and consider constants  $\xi_{cu}, \mu_s, \xi_s, \mu_{cu} \in \mathbb{R}$  satisfying

$$\begin{aligned} \xi_{cu} &\leq m_l \left( \left( \begin{array}{cc} \mathbf{G}_{uu} & \mathbf{G}_{u\theta} \\ \mathbf{G}_{\theta u} & \mathbf{G}_{\theta\theta} \end{array} \right) \right) - L_{cu} \left\| \left( \begin{array}{c} \mathbf{G}_{up} \\ \mathbf{G}_{\theta p} \end{array} \right) \right\|, \\ \mu_s &\geq l(\mathbf{G}_{pp}) + \frac{1}{L_{cu}} \left\| \left( \begin{array}{cc} \mathbf{G}_{pu} & \mathbf{G}_{p\theta} \end{array} \right) \right\|, \\ \xi_s &\leq m_l(-\mathbf{G}_{pp}) - L_s \left\| \left( \begin{array}{cc} \mathbf{G}_{pu} & \mathbf{G}_{p\theta} \end{array} \right) \right\|, \\ \mu_{cu} &\geq l \left( - \left( \begin{array}{cc} \mathbf{G}_{uu} & \mathbf{G}_{u\theta} \\ \mathbf{G}_{\theta u} & \mathbf{G}_{\theta\theta} \end{array} \right) \right) + \frac{1}{L_s} \left\| \left( \begin{array}{c} \mathbf{G}_{up} \\ \mathbf{G}_{\theta p} \end{array} \right) \right\|. \end{aligned}$$

The choice of coordinates for  $Q_{cu}$  is motivated by the fact that the coordinates  $u, \theta$  are center unstable and  $p$  is a stable coordinate for the flow  $\tilde{\Phi}_t$ . The constants  $\xi_{cu}$  and  $\mu_s$  will be used to validate  $Q_{cu}$  cone conditions (see Lemma 22). The choice of coordinates for  $Q_s$  is due to the fact that  $p$  is the unstable and  $u, \theta$  are center stable coordinates for  $\tilde{\Phi}_{-t}$ . The constants  $\xi_s, \mu_{cu}$  and Lemma 23 will be used to validate the backward  $Q_s$  cone conditions and backward outflowing from  $S^u$  along  $Q_s$ .

**Theorem 31.** *Let  $I, R, L_{cu}, L_s, L \in \mathbb{R}$  be fixed and such that  $R, L_{cu} > 0$ ,  $L \in (0, 1)$  and  $L_s \in (0, \pi)$ . Let  $S_{I,L,R}^u$  be an unstable sector for (46) in the energy level  $J = I$ . Assume also that every forward trajectory starting from it must exit the sector and*

$$\xi_{cu} > \mu_s, \quad (50)$$

$$\xi_s > \mu_{cu}, \quad (51)$$

$$\xi_s > 0, \quad (52)$$

*Then, the unstable manifold  $W_{\Lambda_I}^u$  is a graph of a  $Q_{cu}$  center horizontal disc  $w^u : \pi_{u,\theta} S_{I,L,R}^u \rightarrow S_{I,L,R}^u$ , which satisfies  $\pi_{u,\theta} w^u = \text{id}$ , and*

$$|\pi_p(w^u(u_1, \theta_1) - w^u(u_2, \theta_2))| \leq L_{cu} \|(u_1, \theta_1) - (u_2, \theta_2)\|.$$

**Proof.** By Lemma 22 and (50), the flow  $\tilde{\Phi}_t$  induced by  $\tilde{F}$  satisfies forward cone conditions for  $Q_{cu}$  in  $S^u$ . By Lemma 23 and (51–52) the flow satisfies backward cone conditions for  $Q_s$  in  $S^u$  and is backward outflowing from  $S^u$  along  $Q_s$ . The result follows from Theorem 16. ■

We have used Theorem 31 to validate the following result.

**Theorem 32.** *Let*

$$I = -1, \quad L = 4 \cdot 10^{-9}, \quad R = 10^{-4}, \quad L_{cu} = L_s = 10^{-5}.$$

*Then  $S_{I,L,R}^u$  is an unstable sector and the unstable manifold  $W_{\Lambda_I}^u$  is a graph of a  $Q_{cu}$  center horizontal disc in  $S_{I,L,R}^u$ .*

**Proof.** The proof follows by computer assisted validation of the assumptions of Theorems 28 and 31.

In our computer assisted validation, we obtain the following bound of the factorised derivative term  $\mathbf{G}$  from (49),

$$\mathbf{G} = \begin{pmatrix} [0.9999999, 1] & [-2.561\text{e-}08, 1.921\text{e-}09] & [-3.142\text{e-}13, 4.011\text{e-}21] \\ [-3.004\text{e-}09, 1.511\text{e-}07] & [-0.25, -0.2499999] & [-1.003\text{e-}20, 7.854\text{e-}13] \\ [-9.751\text{e-}12, 1.593\text{e-}15] & [-3.903\text{e-}12, 1.050\text{e-}15] & [-1.044\text{e-}20, 2.531\text{e-}20] \end{pmatrix},$$

which results in

$$\begin{aligned} \xi_{cu} &= -5.288\text{e-}12, & \mu_{cu} &= 0.00257, \\ \mu_s &= -0.2348, & \xi_s &= 0.2499999. \end{aligned}$$

Note that  $S_{I,L,R}^u \cup S_{I,L,R}^- \subset \{x > 0, y < 0\}$  (in the “original”  $(x, y)$  coordinates, see (37)). This, by (36), implies that  $\dot{x} > 0$ . This means that every forward trajectory starting from a point in the set  $S_{I,L,R}^u$  must exit the set.

The computer assisted proof takes a fraction of a second, running on a standard laptop. ■

### 5.1. Extending the unstable manifold

The goal of this section is to extend the unstable manifold beyond  $\overline{\pi_{u,p,\theta} S_{I,L,R}^u}$ . We use an argument based on the properties of the vector field, to establish that the unstable manifold of the periodic orbit  $\Lambda_I$  (see (35)) stretches away from  $\Lambda_I$  along the corresponding unstable manifold of the two body problem. In the case when  $\mu$  is small, the unstable manifold of the two body problem proves to be a sufficiently good approximation.

We start with the description of the system for  $\mu = 0$ . In the case of the two body problem the Hamiltonian is given by

$$H(r, \alpha, y, G) = \frac{1}{2} \left( \frac{G^2}{r^2} + y^2 \right) - \frac{1}{r}, \quad (53)$$

(compare with (27)) and the equations of motion are

$$\begin{aligned} \dot{r} &= y, \\ \dot{y} &= \frac{G^2}{r^3} - \frac{1}{r^2}, \\ \dot{\alpha} &= \frac{G}{r^2}, \\ \dot{G} &= 0. \end{aligned}$$

The equations for  $r, y$  form a closed system (with  $G$  being a parameter) and we will focus just on them. We see that

$$\begin{aligned} \dot{r} &= y, \\ \dot{y} &= \frac{G^2}{r^3} - \frac{1}{r^2}. \end{aligned} \quad (54)$$

Let us define an effective potential  $W$  for (54)

$$W(r) = \frac{G^2}{2r^2} - \frac{1}{r}. \quad (55)$$

and an effective hamiltonian for (54)

$$H(r, y) = \frac{y^2}{2} + W(r). \quad (56)$$

We are interested in the parabolic solution (it has  $y \rightarrow 0$  for large  $r$ ), which is a solution with  $H(r, y) = 0$ . We have

$$y = \pm \sqrt{\frac{2}{r} - \frac{G^2}{r^2}} = \pm x \sqrt{1 - \left( \frac{Gx}{2} \right)^2}. \quad (57)$$

where in the last equality we have used McGehee coordinates (29)  $r = 2/x^2$ .

The solution with  $+$  is the stable manifold of the point at infinity (because  $\dot{r} = y > 0$  hence it will grow to infinity) and with  $-$  is the unstable manifold. Since, for  $r \gg 1$  one has  $G \approx -I$ , we expect

$$\gamma_I(x) := -x \sqrt{1 - \left( \frac{Ix}{2} \right)^2} \quad (58)$$

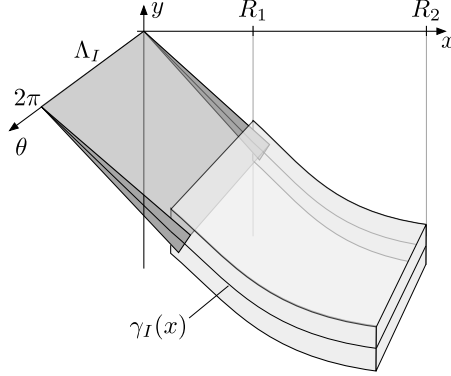


Figure 4: The unstable sector  $S_{I,L,R}^u$  ind dark grey, and its extension  $S_{I,R_1,R_2,\varepsilon}$  in light grey.

to be a good approximation of the unstable manifold in the energy level  $H = I$ , when  $\mu$  is small.

Let  $I$  be fixed. We now extend the sector  $S_{I,L,R}^u$  further away from zero. Let us consider the change of coordinates from  $(x, y, G, \phi)$  to  $(x, \eta, G, \phi)$  defined as

$$y = \gamma_I(x) + \eta.$$

Let  $\mathcal{G}_I(x, \eta, \phi)$  be the solution for  $G$  of the quadratic equation

$$I = \frac{x^4 G^2}{8} + \frac{1}{2} (\gamma_I(x) + \eta)^2 - \mathcal{U}(x, \phi) - G, \quad (59)$$

for given  $x, \eta, \phi$ . Let us now define the following extension of a sector. Let  $R_1, R_2, \varepsilon \in \mathbb{R}$  be such that  $0 < R_1 < R_2$ ,  $\varepsilon > 0$ , and let (see Figure 4)

$$S_{I,R_1,R_2,\varepsilon} := \{(x, \eta, G, \phi) : x \in [R_1, R_2], \phi \in \mathbb{S}^1, G = \mathcal{G}_I(x, \eta, \phi), \eta \in [-\varepsilon, \varepsilon]\}. \quad (60)$$

**Remark 33.** *The earlier considered sector  $S_{I,L,R}^u$  is expressed in the coordinates  $(q, p, G, \theta)$  and is connected with  $\Lambda_I$ . The set  $S_{I,R_1,R_2,\varepsilon}$  is in coordinates  $(x, \eta, G, \phi)$  and is separated from  $\Lambda_I$  since points in this set satisfy  $x \geq R_1$ .*

We now give a theorem which ensures that the unstable manifold passes through  $S_{I,R_1,R_2,\varepsilon}$ .

**Theorem 34.** *Let all assumptions of Theorem 31 be fulfilled. Let*

$$\begin{aligned} F_x(x, \eta, \phi) &:= -\frac{1}{4} x^3 (\gamma_I(x) + \eta), \\ F_\eta(x, \eta, \phi) &:= \frac{1}{8} x^6 (\mathcal{G}_I(x, \eta, \phi))^2 - \frac{x^3}{4} \frac{\partial \mathcal{U}}{\partial x}(x, \phi) \\ &\quad + \frac{\partial \gamma_I}{\partial x}(x) \frac{1}{4} x^3 (\gamma_I(x) + \eta), \end{aligned}$$

*Assume that there exist  $\varepsilon > 0$  and  $R_1, R_2 \in \mathbb{R}$ ,  $0 < R_1 < R_2$ , for which the following conditions hold:*

1. The set  $\overline{S_{I,L,R}^u} \cap \{q = R\}$  is a subset of  $S_{I,R_1,R_2,\varepsilon}$ ; i.e. if  $(q, p, G, \theta) \in \overline{S_{I,L,R}^u}$  and  $q = R$  then

$$(p + q, p - q - \gamma_I(p + q), G, \theta - G(p - q)) \in S_{I,R_1,R_2,\varepsilon}.$$

2. We have

$$\begin{aligned} F_\eta(x, \varepsilon, G, \phi) &< 0 && \text{for every } (x, \varepsilon, G, \phi) \in S_{I,R_1,R_2,\varepsilon}, \\ F_\eta(x, -\varepsilon, G, \phi) &> 0 && \text{for every } (x, -\varepsilon, G, \phi) \in S_{I,R_1,R_2,\varepsilon}. \end{aligned}$$

3. For every  $(x, \eta, G, \phi) \in S_{I,R_1,R_2,\varepsilon}$ ,

$$F_x(x, \eta, G, \phi) > 0.$$

Then, every point from  $W_{\Lambda_I}^u \cap \{q = R\}$  is contained in  $S_{I,R_1,R_2,\varepsilon}$  and the flow starting from such point exits  $S_{I,R_1,R_2,\varepsilon}$  through  $\{x = R_2\}$ .

**Proof.** Since  $S_{I,L,R}^u$  is an unstable sector, by Theorem 31 it contains the unstable manifold  $W^u$ . The first condition therefore ensures that all points on  $W^u \cap \{q = R\}$  are inside of  $S_{I,R_1,R_2,\varepsilon}$ . The  $F_\eta$  is the the vector field on the coordinate  $\eta$ , so the second condition ensures that trajectories starting from  $W^u \cap \{q = R\}$  cannot exit  $S_{I,R_1,R_2,\varepsilon}$  through  $\{\eta = \varepsilon\}$  or  $\{\eta = -\varepsilon\}$ . Since  $F_x$  is the vector field on the coordinate  $x$ , the third condition ensures that the coordinate  $x$  increases along the flow. This means that a trajectory starting from  $W^u \cap \{q = R\}$  has to exit  $S_{I,R_1,R_2,\varepsilon}$  through  $\{x = R_2\}$ . ■

We have used Theorem 34 to validate the following result:

**Theorem 35.** *Let*

$$I = -1, \quad L = 4 \cdot 10^{-9}, \quad R = 10^{-4}, \quad R_1 = \frac{R}{2}, \quad R_2 = 0.4, \quad \varepsilon = 2 \cdot 10^{-5}.$$

Then, every point from  $W_{\Lambda_I}^u \cap \{q = R\}$  is contained in  $S_{I,R_1,R_2,\varepsilon}$  and the flow starting from such point exits  $S_{I,R_1,R_2,\varepsilon}$  through  $\{x = R_2\}$ .

**Proof.** The conditions to apply Theorem (34) can be validated by subdividing  $S_{I,R_1,R_2,\varepsilon}$  into  $10^5$  pieces along the coordinate  $x$  and into 50 pieces along the coordinate  $\phi$  (in total  $5 \cdot 10^6$  pieces) and by checking the required conditions on each of the ‘‘cubes’’ separately. Such computation took under two minutes on a standard laptop. ■

## 6. Proof of the main Theorem

Here we shall construct oscillatory motions and, therefore, prove Theorem 1.

Throughout this section we will be working under the assumption that we have a setting in which there is an unstable sector  $S_{I,L,R}^u$  which is established by means of Lemma 28. Moreover, we shall assume that the unstable manifold within it is established by means of Theorem 31. We will also assume that the bound on the manifold is extended to  $S_{I,R_1,R_2,\varepsilon}$  by means of Theorem 34.

Since  $S_{I,L,R}^u \cup S_{I,R_1,R_2,\varepsilon} \subset \{x > 0, y < 0\}$  by (36) we see that on  $S_{I,L,R}^u \cup S_{I,R_1,R_2,\varepsilon}$  we have  $\dot{x} > 0$ . This means that if there is a point in  $S_{I,L,R}^u \cup S_{I,R_1,R_2,\varepsilon}$  whose backward trajectory remains in this set, then it has to converge to  $\Lambda_I$  (See Figure 4).

**Remark 36.** For the energy level  $H = I$  with  $I = -1$  we have validated the existence of  $S_{I,L,R}^u$  and of  $S_{I,R_1,R_2,\varepsilon}$  by means of a computer assisted (see Theorems 32 and 35).

Due to the symmetry property of system (33) from the bound on the unstable manifold we automatically obtain the bound  $\mathcal{S}(S_{I,L,R}^u \cup S_{I,R_1,R_2,\varepsilon})$  on the stable manifold.

The oscillatory motions will be established by the method of covering relations [19, 26]. We start by recalling the method, and then apply it to our problem in the subsequent section.

### 6.1. Covering relations

We restrict to the case of covering relations for maps on  $\mathbb{R}^2$ , since this is sufficient for our application. This allows us to simplify some of the introduced tools and notions. The methods from [19, 26] though, are general and can be applied to carry out analogous constructions in higher dimensional settings.

**Definition 37.** An h-set is a pair  $(N, c_N)$  where  $N \subset \mathbb{R}^2$  and  $c_N : \mathbb{R}^2 \rightarrow \mathbb{R}^2$  is a homeomorphism such that  $c_N(N) = [-1, 1] \times [-1, 1]$ .

For simplicity, when referring to an h-set we will sometimes write only the set  $N$ , always assuming implicitly that we have an associated homeomorphism  $c_N$  with it.

For an h-set  $(N, c_N)$  we define

$$\begin{aligned} N_c &= [-1, 1] \times [-1, 1], \\ N_c^l &= \{-1\} \times [-1, 1], \\ N_c^r &= \{1\} \times [-1, 1], \\ N_c^- &= N_c^l \cup N_c^r, \\ N_c^+ &= ([-1, 1] \times \{-1\}) \cup ([-1, 1] \times \{1\}), \end{aligned}$$

and

$$N^l = c_N^{-1}(N_c^l), \quad N^r = c_N^{-1}(N_c^r), \quad N^- = c_N^{-1}(N_c^-), \quad N^+ = c_N^{-1}(N_c^+).$$

In this section we use the notation  $(x, y) \in N_c \subset \mathbb{R}^2$  for the coordinates. We write  $\pi_x$  and  $\pi_y$  for the projections onto the x and y coordinates, respectively. Note that we use a different font x, y in order to distinguish these with the coordinates  $x, y$  of the PCR3BP.

**Definition 38.** Let  $(M, c_M)$  and  $(N, c_N)$  be two h-sets. Let  $f : \mathbb{R}^2 \rightarrow \mathbb{R}^2$  be a continuous map and let  $f_c := c_N \circ f \circ c_M^{-1}$ . We say that  $(M, c_M)$  f-covers  $(N, c_N)$ , which we denote as

$$M \xrightarrow{f} N,$$

iff

$$\pi_x f_c(M_c^l) < -1 \quad \text{and} \quad \pi_x f_c(M_c^r) > 1, \quad (61)$$

or

$$\pi_x f_c(M_c^r) < -1 \quad \text{and} \quad \pi_x f_c(M_c^l) > 1, \quad (62)$$

and

$$\pi_y f_c(M_c) \cap ([-1, 1] \times (\mathbb{R} \setminus (-1, 1))) = \emptyset. \quad (63)$$

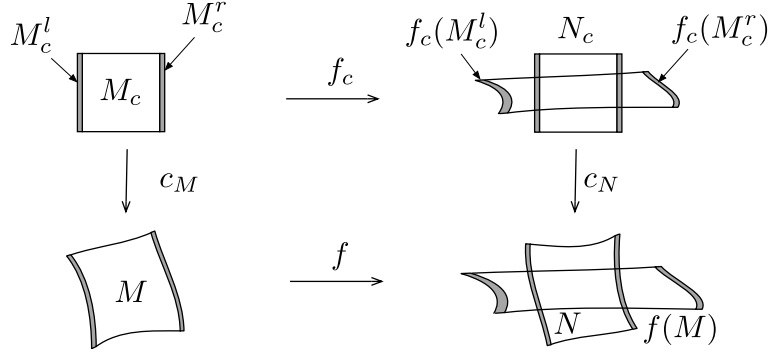


Figure 5: The covering  $M \xrightarrow{f} N$ .

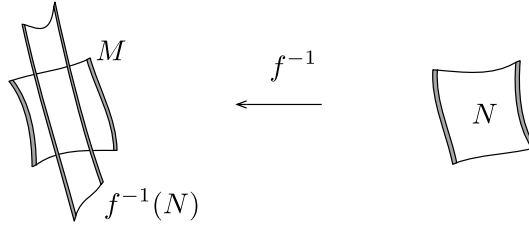


Figure 6: The back-covering  $M \xleftarrow{f} N$ .

The coordinate  $x$  plays the role of a local coordinate along which we have a topological expansion, and  $y$  plays the role of a coordinate along which we have a topological contraction.

We now introduce the notion of back-covering.

**Definition 39.** Let  $T : \mathbb{R}^2 \rightarrow \mathbb{R}^2$  be defined as  $T(x, y) = (y, x)$ . For an  $h$ -set  $(N, c_N)$  we define an  $h$ -set  $(N^T, c_N^T)$  as

$$\begin{aligned} N^T &= N, \\ c_N^T &= T \circ c_N. \end{aligned}$$

**Definition 40.** Let  $(M, c_M)$  and  $(N, c_N)$  be two  $h$ -sets. Let  $f : \mathbb{R}^2 \rightarrow \mathbb{R}^2$  be a continuous and such that  $f^{-1} : N \rightarrow \mathbb{R}^2$  is well defined. We say that  $(M, c_M)$   $f$ -back-covers  $(N, c_N)$ , which we denote as

$$M \xleftarrow{f} N,$$

iff

$$N^T \xrightarrow{f^{-1}} M^T.$$

For our shadowing theorem we also need the following notions.

**Definition 41.** Let  $N$  be an  $h$ -set. Let  $h : [-1, 1] \rightarrow N$  be continuous and let  $h_c = c_N \circ h$ . We say that  $h$  is a horizontal disk in  $N$  if

$$\pi_x h_c(x) = x.$$

**Definition 42.** Let  $N$  be an  $h$ -set. Let  $v : [-1, 1] \rightarrow N$  be continuous and let  $v_c = c_N \circ v$ . We say that  $v$  is a vertical disk in  $N$  if

$$\pi_y v_c(y) = y.$$

**Definition 43.** Let  $N$  be an  $h$ -set and  $h$  and  $v$  be horizontal and vertical discs in  $N$ , respectively. By  $|h|$  and  $|v|$  we denote the image of  $h$  and  $v$ , respectively.

The theorem below is our main tool for establishing oscillatory motions.

**Theorem 44.** [19, Thm. 4][26, Thm. 4] Let  $k \geq 1$ . Assume that  $N_i$ ,  $i = 0, \dots, k$ , are  $h$ -sets and for each  $i = 1, \dots, k$  we have either

$$N_{i-1} \xrightarrow{f_i} N_i \tag{64}$$

or

$$N_{i-1} \xleftarrow{f_i} N_i. \tag{65}$$

1. If  $N_k = N_0$  then there exists an  $x \in \text{int}N_0$  such that

$$f_i \circ f_{i-1} \circ \dots \circ f_1(x) \in \text{int}N_i \quad \text{for every } i \in \{1, \dots, k\},$$

and

$$f_k \circ f_{k-1} \circ \dots \circ f_1(x) = x.$$

2. Let  $h$  be a horizontal disk in  $N_0$  and  $v$  a vertical disk in  $N_k$ . Then there exists a point  $z \in \text{int}N_0$ , such that

$$\begin{aligned} z &\in |h|, \\ f_i \circ f_{i-1} \circ \dots \circ f_1(z) &\in \text{int}N_i, \quad i = 1, \dots, k \\ f_k \circ f_{k-1} \circ \dots \circ f_1(z) &\in |v|. \end{aligned} \tag{66}$$

**Corollary 45.** We have the following results for infinite sequences of coverings:

1. If

$$N_{i-1} \xrightarrow{f_i} N_i \quad \text{or} \quad N_{i-1} \xleftarrow{f_i} N_i \quad \text{for } i = 1, 2, \dots$$

then, for every horizontal disc  $h$  in  $N_0$ , there exists a forward trajectory  $z_0, z_1, \dots$ ,  $f_i(z_{i-1}) = z_i$ , such that  $z_i \in \text{int}N_i$  for  $i = 1, 2, \dots$  and  $z_0 \in |h|$ .

2. If

$$N_{i-1} \xrightarrow{f_i} N_i \quad \text{or} \quad N_{i-1} \xleftarrow{f_i} N_i \quad \text{for } i = 0, -1, -2, \dots$$

then, for every vertical disc  $v$  in  $N_0$ , there exists a backward trajectory  $\dots, z_{-2}, z_{-1}, z_0$ ,  $f_i(z_{i-1}) = z_i$ , such that  $z_i \in \text{int}N_i$  for  $i = -1, -2, \dots$  and  $z_0 \in |v|$ .

3. If

$$N_{i-1} \xrightarrow{f_i} N_i \quad \text{or} \quad N_{i-1} \xleftarrow{f_i} N_i \quad \text{for } i \in \mathbb{Z},$$

there exists full trajectory  $(z_i)_{i \in \mathbb{Z}}$ ,  $f_i(z_{i-1}) = z_i$ , such that  $z_i \in \text{int}N_i$  for  $i \neq 0$  and  $z_0 \in N_0$ .

**Proof.** For item 1, from Theorem 44 and a finite sequence of coverings

$$N_{i-1} \xrightarrow{f_i} N_i \quad \text{or} \quad N_{i-1} \xleftarrow{f_i} N_i \quad \text{for } i = 0, 1, \dots, k,$$

we obtain  $x_k \in |h|$ , such that a trajectory starting from  $x_k$  visits the successive h-sets  $N_i$ ,  $i = 1 \dots k$ . By compactness of  $|h|$ , there exists a convergent subsequence  $x_{k_i} \xrightarrow{i \rightarrow \infty} z_0 \in |h|$ , which proves our claim.

Items 2 and 3 follow from mirror arguments. Item 2 follows by considering finite sequences with  $i \in \{-k, \dots, -1, 0\}$  and Item 3 by considering finite sequences with  $i \in \{-k, \dots, k\}$ . ■

### 6.2. Overview of the proof

The proof will be based on a construction of appropriate h-sets, which will be positioned on two dimensional sections along the flow. Note that we fix the energy level at  $H = I$ , which makes the system three dimensional, so sections transversal to the flow are of dimension two. We consider three sections on which we will position our h-sets

$$\begin{aligned} \Sigma_0 &= \{y = 0\}, \\ \Sigma_1 &= \{x = R_2\}, \\ \Sigma &= \{\phi = 0\}, \end{aligned}$$

where  $R_2 \in \mathbb{R}$  is a fixed constant (as obtained in Theorem 35). On these sections we consider several types of h-sets:

$$\begin{aligned} N_0 &\subset \Sigma_0, \\ N_1 &\subset \Sigma_1, \\ N(r), N(\bar{r}, r), M(\alpha, \beta) &\subset \Sigma. \end{aligned}$$

(The  $r, \bar{r}, \alpha, \beta$  are parameters. The set  $N_0$  is defined in (70) and depicted in Figure 7; the set  $N_1$  is defined in (71); The set  $N(r)$  is defined in (72) and depicted in Figure 8; The set  $N(\bar{r}, r)$  is defined in (75) and depicted in Figure 9; The set  $M(\alpha, \beta)$  is defined in (77) and depicted in Figure 10. The smaller the  $r, \bar{r}, \alpha, \beta$  the closer the h-sets are to  $\Lambda_I$ .)

Set  $N_0$  is self  $\mathcal{S}$ -symmetric (see Figure 7). Checking that

$$N_1 \implies N_0$$

involves computer assisted validation. The rest of coverings is proven by analytic arguments. The smaller the parameter  $r$ , the closer the left side of the exit set of  $N(r)$  is to  $\Lambda_I$ ; see Figure 8. This will allow us to prove in Lemma 51 that if  $r$  is sufficiently small then

$$N(r) \implies N_1.$$

In Lemma 54 we prove that

$$N(\bar{r}, r) \implies N(r),$$

provided that we choose appropriately small  $\bar{r}$ . We also show in Lemmas 56, 57 that we have a sequence of coverings

$$M(\bar{r}, r) \implies M(\alpha, \beta) \implies N(\bar{r}, r),$$

for arbitrarily small  $\alpha, \beta$ . The smaller we choose  $\alpha, \beta$  the closer to  $\Lambda_I$  is the h-set  $M(\alpha, \beta)$ . This means that we can obtain an orbit that passes through the above sequence of coverings to approach arbitrarily close to  $\Lambda_I$ . The set  $M(\bar{r}, r)$  is an  $\mathcal{S}$ -symmetric to  $N(\bar{r}, r)$ , this allows us to automatically obtain coverings from  $N_0$  to  $M(\bar{r}, r)$ , this way we obtain a sequence of coverings

$$N_0 \implies \dots \implies M(\alpha, \beta) \implies \dots \implies N_0. \quad (67)$$

The smaller the  $\alpha, \beta$  the closer is the approach to  $\Lambda_I$  for orbits that pass through such sequences. We then choose a sequence  $M(\alpha_1, \beta_1), M(\alpha_2, \beta_2), \dots$  and glue sequences (67) to obtain oscillatory motions.

To prove bounded motions we will glue infinite sequences (67) with fixed  $\alpha = \bar{r}$  and  $\beta = r$ .

To prove parabolic and hyperbolic motions, we will choose appropriate horizontal discs in  $N(\bar{r}, r)$  and vertical discs in  $M(\bar{r}, r)$  and use the connection

$$N(\bar{r}, r) \implies \dots \implies N_0 \implies \dots \implies M(\bar{r}, r).$$

The discs will be chosen so that when an orbit passes through a given disc, it escapes to infinity (i.e.  $x = 0$  in McGehee variables (29)) according to a given type of motion (hyperbolic or parabolic).

### 6.3. Proof of the main theorem

Throughout this section we consider

$$I = -1, \quad L = 4 \cdot 10^{-9}, \quad R = 10^{-4}, \quad R_1 = \frac{R}{2}, \quad R_2 = 0.4, \quad \varepsilon = 2 \cdot 10^{-5},$$

as in Theorems 32 and 35. We focus on the case  $I = -1$ , but the method is general and can be applied to different energy levels (i.e. values of the Jacobi constant).

Our objective is to construct a sequence of h-sets, positioned on sections along the flow of the PCR3BP. Our objective is to define these h-sets, so that Theorem 44 will lead to the existence of orbits which can approach arbitrarily close to infinity and come back to the regions of the primaries.

Let  $\mathcal{G}_I(x, y, \phi)$  be defined as

$$\mathcal{G}_I(x, y, \phi) := \frac{1 - \sqrt{1 - \frac{x^4}{2} \left( \frac{1}{2}y^2 - \mathcal{U}(x, \phi) - I \right)}}{\frac{x^4}{4}} \quad (68)$$

a solution of the quadratic equation

$$I = \frac{x^4 G^2}{8} + \frac{1}{2}y^2 - \mathcal{U}(x, \phi) - G.$$

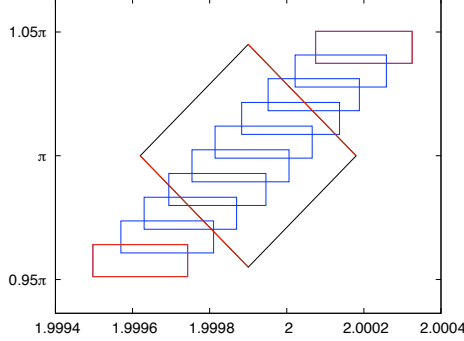


Figure 7: The covering  $N_1 \xrightarrow{f_0} N_0$ . The set  $N_0$  is the rhombus, with the exit set marked in red. The computer assisted bound on the image of  $N_1$  is depicted by the diagonally placed rectangles, and the bound on the exit set is depicted in red. The figure is in the  $(x, \phi)$  coordinates, with  $x$  on the horizontal axis and  $\phi$  on the vertical axis.

Note that  $\lim_{(x,y) \rightarrow (0,0)} \mathcal{G}_I(x, y, \phi) = -I$  and

$$\mathcal{G}_I(x, y, \phi) = \mathcal{G}_I(x, -y, -\phi). \quad (69)$$

We consider the first h-set on the section  $\Sigma_0 = \{y = 0\}$ . We consider the flow restricted to energy level  $H = I$ , which means that  $\Sigma_0$  is two dimensional. The points on this section are parametrised by  $x$  and  $\phi$ , since the coordinate  $G$  is determined by (68). We will therefore specify an h-set on  $\Sigma_0$  in coordinates  $x, \phi$ .

To define our first h-set  $N_0$  we consider two matrices  $S_{\alpha, \beta}$  and  $\mathcal{R}$  as

$$S_{\alpha, \beta} := \text{diag}(\alpha, \beta), \quad \mathcal{R} := \begin{pmatrix} \cos\left(\frac{\pi}{4}\right) & -\sin\left(\frac{\pi}{4}\right) \\ \sin\left(\frac{\pi}{4}\right) & \cos\left(\frac{\pi}{4}\right) \end{pmatrix}$$

with which we define

$$\begin{aligned} N_0 &:= S_{\alpha, \beta} \circ \mathcal{R}([-1, 1] \times [-1, 1]) + (x_0, \pi), \\ c_{N_0}(z) &:= \mathcal{R}^{-1} S_{\alpha, \beta}^{-1}(z - (x_0, \pi)), \end{aligned} \quad (70)$$

where  $\alpha, \beta, x_0$  are given parameters. We have found that good choices of the parameters are

$$\alpha = 2 \cdot 10^{-4}, \quad \beta = 10^{-1}, \quad x_0 = 1.9999.$$

The choice of  $x_0$  is motivated by the fact that the point  $(x_0, \pi)$  is (roughly) on the intersection of the stable and unstable manifolds at  $\Sigma_0$ . The set  $N_0$  is constructed by rotating counterclockwise the square  $[-1, 1]^2$  by the angle  $\frac{\pi}{4}$ , rescaling it, and shifting it to be centered at  $(x_0, \pi)$ . This way we obtain a rhombus depicted in Figure 7. The scaling coefficients  $\alpha, \beta$  are chosen so that the edges  $N^+$  are (roughly) aligned with the intersection of the unstable manifold with  $\Sigma_0$ . In Figure 7 the (rigorous, computer-assisted) bound on this intersection is depicted in blue.

**Remark 46.** The set  $N_0$  is  $\mathcal{S}$  symmetric. To be more precise, if  $(x, y = 0, \phi, G) \in \Sigma_0$  is a point in  $N_0$  then

$$\mathcal{S}(x, 0, \phi, G) = (x, 0, -\phi, G)$$

lies in  $\{y = 0\}$ . The point  $(x, -\phi)$  lies in the rhombus, since  $-\phi$  is identified with  $-\phi + 2\pi$ , and the rhombus is symmetric with respect to the line  $\phi = \pi$  (see Figure 7), and from (69) we see that  $\mathcal{S}(x, 0, \phi, G) \in N_0 \subset \Sigma_0$ .

Our second h-set  $N_1$  is contained in the section

$$\Sigma_1 = \{x = R_2\}.$$

The points on  $\Sigma_1$  are parameterised by  $\phi, y$ , since  $G$  can be computed as  $G = \mathcal{G}_I(R_2, y, \phi)$ . On the section  $\Sigma_1$  the role of the exit coordinate is played by  $\phi$ , and the topologically entry coordinate is  $y$ . We consider the set  $N_1 \subset \Sigma_1$ , defined on the  $\phi, y$  coordinates as

$$N_1 = [\phi_1, \phi_2] \times [\gamma_I(R_2) - \varepsilon, \gamma_I(R_2) + \varepsilon], \quad (71)$$

where good choices of parameters  $\phi_1, \phi_2$  are

$$\phi_1 = 3.45 \quad \text{and} \quad \phi_2 = 3.75.$$

We consider  $f_0 : \Sigma_1 \rightarrow \Sigma_0$  to be the section to section map along the flow of the PCR3BP. With the aid of computer assisted computation we validate the following result.

**Lemma 47.** For  $I = -1$  and the above defined h-sets  $N_0, N_1$  and the section to section map  $f_0 : \Sigma_1 \rightarrow \Sigma_0$  we have

$$N_1 \xrightarrow{f_0} N_0.$$

**Proof.** The computer assisted bounds that validate Lemma 47 are depicted in Figure 7. The computation took under eight seconds on a standard laptop. ■

**Corollary 48.** Let  $\tilde{f}_0 : \Sigma_0 \rightarrow \Sigma_1$  be section to section map along the flow of the PCR3BP (for positive time). From the time reversing symmetry (33) we obtain that (recall that  $N^T$  was defined in Definition 40)

$$N_0 \xleftarrow{\tilde{f}_0} \mathcal{S}(N_1^T).$$

**Remark 49.** The computation for the proof of Lemma 47, see Figure 7, shows that the stable and unstable manifolds of  $\Lambda_I$  intersect. This follows from the fact that these manifolds are  $\mathcal{S}$ -symmetric.

We choose our next h-set on the section

$$\Sigma = \{\phi = 0\}.$$

The points on  $\Sigma$  are parameterised by  $x, y$ , since  $G$  can be computed as  $G = \mathcal{G}_I(x, y, 0)$ . On  $\Sigma$  we can therefore consider h-sets expressed in coordinates  $x, y$ . The coordinate  $y$  is entry direction and  $x$  is the exit direction. We define the following h-set,  $N(r)$ , where

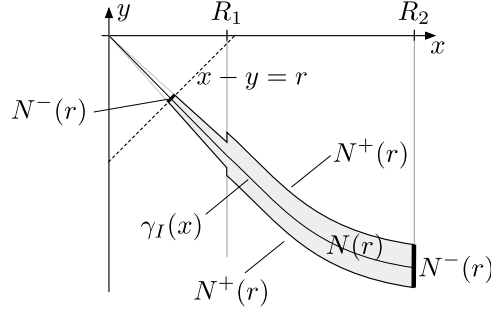


Figure 8: The h-set  $N(r)$ .

$r \in (0, R)$  and (for the intuition behind the definition see Figure 8 and the explanation that comes in the next paragraph)

$$N(r) := \{(x, y) : x \in [R_1, R_2] \text{ and } y \in [\gamma_I(x) - \varepsilon, \gamma_I(x) + \varepsilon]\} \cup \{(x, y) : x < R_1, x - y \geq r \text{ and } |x + y| \leq L(x - y)\}. \quad (72)$$

The reason for above definition of  $N(r)$  is the following. For  $x \in [R_1, R_2]$ , from the definition of  $S_{I, R_1, R_2, \varepsilon}$  we know that the unstable manifold on  $\Sigma$  is enclosed in an  $\varepsilon$  neighbourhood of the curve  $(x, \gamma_I(x))$ . We therefore position our h-set around this curve for  $x \in [R_1, R_2]$ . Recall also that the coordinates  $q, p$  were defined as  $q = \frac{1}{2}(x - y)$  and  $p = \frac{1}{2}(x + y)$ , so the condition  $|x + y| \leq L|x - y|$  ensures that  $|p| \leq Lq$ , so the points in  $N(r)$  that have  $x < R_1$  lie in the sector  $S_{I, L, R}^u$ .

The sets  $N^\pm(r)$  are depicted on Figure 8. The formal definition is follows

$$\begin{aligned} N^+(r) &= \{(x, y) : x \in [R_1, R_2] \text{ and } y = \gamma_I(x) - \varepsilon\} \\ &\cup \{(x, y) : x \in [R_1, R_2] \text{ and } y = \gamma_I(x) + \varepsilon\} \\ &\cup \left\{ (x, y) : x = R_1, -x(1-L)(1+L)^{-1} \leq y \text{ and } y \leq \gamma_I(x) + \varepsilon \right\} \\ &\cup \left\{ (x, y) : x = R_1, \gamma_I(x) - \varepsilon \leq y \text{ and } y \leq -x(1+L)(1-L)^{-1} \right\} \\ &\cup \{(x, y) : x \leq R_1, x - y \geq r, \text{ and } |x + y| = L(x - y)\}, \\ N^-(r) &= \{(x, y) : x = R_2 \text{ and } y \in [\gamma_I(x) - \varepsilon, \gamma_I(x) + \varepsilon]\} \\ &\cup \{(x, y) : x - y = r, \text{ and } |x + y| \leq L(x - y)\}. \end{aligned}$$

Let us assume that for every point from the set

$$\{(x, y, \phi, G) : (x, y) \in N(r), \phi \in \mathbb{S}^1, G = \mathcal{G}_I(x, y, \phi)\}$$

we have (see (36))

$$\dot{\phi} < 0. \quad (73)$$

**Remark 50.** For a given fixed  $I$  (73) can be validated with the aid of a computer and interval arithmetic.

Let

$$f_1 : \Sigma \rightarrow \Sigma_1$$

be the section to section map along the flow.

**Lemma 51.** *There exists an  $r_0 > 0$  such that for any  $r \in (0, r_0)$*

$$N(r) \xrightarrow{f_1} N_1.$$

**Proof.** The flow starting from any point in  $N(r)$  will remain in the interior of  $S_{I,L,R}^u \cup S_{I,R_1,R_2,\varepsilon}$  until it exits this set through  $\Sigma_1 = \{x = R_2\}$ . This means that the trajectory will not pass through  $N_1^+ = \{y = \gamma_I(R_2) \pm \varepsilon, \phi \in [\phi_1, \phi_2]\}$  (see (71)), so

$$\pi_y f_1(N(r)) \cap N_1^+ = \emptyset,$$

which validates condition (63) from the definition of the covering relation.

Let us now observe that

$$N^-(r) \cap \{x = R_2\} \in \Sigma_1.$$

This means that

$$f_1(p) = p, \quad \text{for every } p \in N^-(r) \cap \{x = R_2\},$$

which implies

$$\pi_\phi f_1(p) = 0 \quad \text{for every } p \in N^-(r) \cap \{x = R_2\}. \quad (74)$$

Observe that since  $\phi_1, \phi_2$  used to define  $N_1$  are such that zero is not within the interval  $[\phi_1, \phi_2]$ . This means that from (74) we obtain

$$f_1(N^-(r) \cap \{x = R_2\}) \cap N_1 = \emptyset.$$

Let us now consider  $\phi$  to be from  $\mathbb{R}$  instead of  $\mathbb{S}^1$ . In other words, we consider a lift of the angle to the real line. From (73) we see that  $\pi_\phi f_1(N(r)) \in \mathbb{R}_-$ . We can identify  $N_1$  with  $[\phi_1 - 2\pi, \phi_2 - 2\pi] \times [\gamma_I(R_2) - \varepsilon, \gamma_I(R_2) + \varepsilon]$  so the angles of  $N_1$  are negative. From (74) we see that

$$\pi_\phi f_1(N^-(r) \cap \{x = R_2\}) > \pi_\phi N_1,$$

which is the second inequality of (62), from the definition of the covering relation.

We now need to show that if we choose  $r > 0$  to be sufficiently small, then we will obtain

$$\pi_\phi f_1(N^-(r) \setminus \{x = R_2\}) < \pi_\phi N_1.$$

This establishes the second inequality from (62). The smaller the  $r$  we choose, the closer to the origin, which by  $\dot{\phi}$  in (36) implies that we will have a larger change in  $\phi$  until we reach  $\{x = R_2\}$  from  $\{x - y = r\}$ . Choosing small  $r$  we can therefore obtain  $\pi_\phi f_1(N^-(r) \setminus \{x = R_2\}) < \phi_1 - 2\pi$ , which concludes our proof. ■

**Corollary 52.** *Let  $\tilde{f}_1 : \Sigma_1 \rightarrow \Sigma$  be the section to section map along the flow of the PCR3BP. From the time reversing symmetry (33) and from Lemma 51 we obtain that*

$$\mathcal{S}(N_1^T) \xleftarrow{\tilde{f}_1} \mathcal{S}(N^T(r)).$$

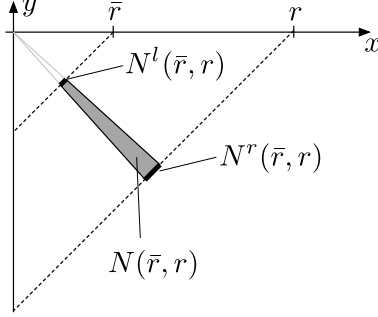


Figure 9: The h-set  $N(\bar{r}, r)$ .

Let  $\bar{r} \in (0, r)$ . Recall that the section  $\Sigma = \{\phi = 0\}$  is parameterised by coordinates  $x, y$ . We define the following h-set  $N(\bar{r}, r)$  in  $\Sigma$  as (see Figure 9).

$$N(\bar{r}, r) = \{(x, y) : x - y \in [\bar{r}, r] \text{ and } |x + y| \leq L(x - y)\}, \quad (75)$$

and

$$\begin{aligned} N^+(\bar{r}, r) &= N(\bar{r}, r) \cap \{(x, y) : |x + y| = L(x - y)\}, \\ N^l &= N(\bar{r}, r) \cap \{x - y = \bar{r}\}, \\ N^r &= N(\bar{r}, r) \cap \{x - y = r\}. \end{aligned}$$

Our objective now will be to show that if  $\bar{r}$  is chosen to be sufficiently small, then we can construct a covering

$$N(\bar{r}, r) \implies N(r).$$

The above statement is vague, since we have not specified which map we consider for the covering. We make this more precise in the discussion that follows.

We first note that for every point in  $S_{I, R_1, R_2, \varepsilon}$  we have  $\dot{x} > 0$ . This means that there exists a  $\delta > 0$ , such that a trajectory that exits  $S_{I, R_1, R_2, \varepsilon}$  will reach  $\{x = R_2 + \delta\}$  without re-entering  $S_{I, R_1, R_2, \varepsilon}$ . Let such  $\delta$  be fixed from now on.

Let  $\tau : \mathbb{R}^2 \times \mathbb{S}^1 \times \mathbb{R} \rightarrow \mathbb{R}$  be defined as

$$\tau(\mathbf{x}) = \min(\inf\{t > 0 : \pi_\phi \Phi_t(\mathbf{x}) = 0\}, \inf\{t \geq 0 : \pi_x \Phi_t(\mathbf{x}) = R_2 + \delta\}),$$

and let  $f : \Sigma \rightarrow \Sigma$  be defined as

$$f(\mathbf{x}) := (\pi_{x,y} \Phi_{\tau(\mathbf{x})}(\mathbf{x}), 0, \mathcal{G}_I(\pi_{x,y} \Phi_{\tau(\mathbf{x})}(\mathbf{x}), 0)).$$

**Remark 53.** From the definition of  $\tau$  we see that if  $\pi_x f(\mathbf{x}) < R_2 + \delta$ , then  $f(\mathbf{x}) = \Phi_{\tau(\mathbf{x})}(\mathbf{x})$ . This means that every point  $\mathbf{x}$  in  $\{x < R_2 + \delta\}$  whose image  $f(\mathbf{x})$  lands in  $\{x < R_2 + \delta\}$ , the map  $f$  corresponds to a true trajectory of the PCR3BP.

The definition of  $f$  is somewhat artificial, but there is a reason for which we choose it this way. When we take  $\mathbf{x} \in S_{I, L, R}^u \cup S_{I, R_1, R_2, \varepsilon}$ , then from the way we have defined  $f$  each iterate  $f^n(\mathbf{x})$  is well defined for every  $n \in \mathbb{N}$ . Moreover, as long as  $\pi_x f^i(\mathbf{x}) \leq R_2$ , for  $i = 0, \dots, n$ , by Remark 53 the points  $f^i(\mathbf{x})$  lie on a trajectory of the PCR3BP.

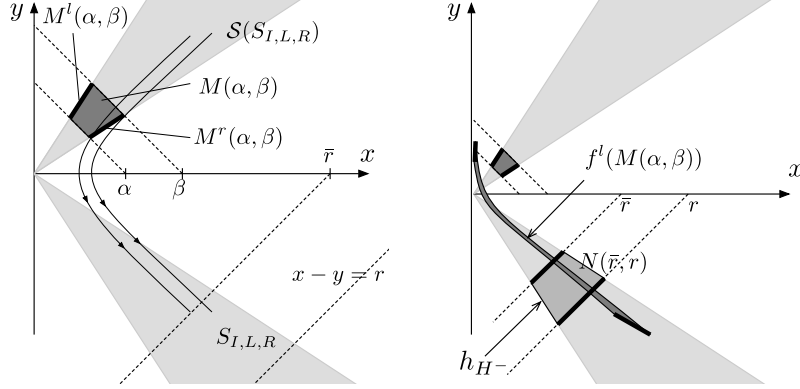


Figure 10: The h-set  $M(\alpha, \beta)$  is in dark grey on the left hand side plot. We see that the exit set  $M^r(\alpha, \beta)$  will enter the sector  $S_{I,R,L}$ . On the right is a sketch of the covering of  $N(\bar{r}, r)$  by  $M(\alpha, \beta)$ .

**Lemma 54.** *For every small enough  $r > 0$  there exists a  $k \in \mathbb{N}$  and  $\bar{r} \in \mathbb{R}$  such that*

$$N(\bar{r}, r) \xrightarrow{f^k} N(r). \quad (76)$$

**Proof.** All trajectories which start from  $S_{I,R,L} \cup S_{I,R_1,R_2,\varepsilon}$  will exit this set through  $S_{I,R_1,R_2,\varepsilon} \cap \{x = R_2\}$ . This means that there exists a  $k$  such that  $\pi_x f^k(N^r(\bar{r}, r)) > R_2$ . This means that the first inequality from the condition (61) needed for (76) will be satisfied. The smaller the  $\bar{r}$ , the closer the points from  $N^l(\bar{r}, r)$  will be to the origin, where the dynamics is slow. This means that by choosing  $\bar{r}$  sufficiently small, we will obtain  $\pi_x f^k(N^l(\bar{r}, r)) < \pi_x N(r)$ , which means that the second inequality from the condition (61) is also satisfied.

We need to show that  $f^k(N(\bar{r}, r)) \cap N^+(r) = \emptyset$ . This follows from the fact that points can exit  $S_{I,R,L} \cup S_{I,R_1,R_2,\varepsilon}$  only through  $S_{I,R_1,R_2,\varepsilon} \cap \{x = R_2\}$ . No trajectory which starts in  $S_{I,R,L} \cup S_{I,R_1,R_2,\varepsilon}$  can therefore pass through  $N^+(r)$ . ■

Let  $\tilde{\tau} : \mathbb{R}^2 \times \mathbb{S}^1 \times \mathbb{R} \rightarrow \mathbb{R}$  be defined as

$$\tilde{\tau}(\mathbf{x}) = \max(\sup\{t < 0 : \pi_\phi \Phi_t(\mathbf{x}) = 0\}, \sup\{t \leq 0 : \pi_x \Phi_t(\mathbf{x}) = R_2 + \delta\}),$$

and let  $\tilde{f} : \Sigma \rightarrow \Sigma$  be defined as

$$\tilde{f}(\mathbf{x}) := (\pi_{x,y} \Phi_{\tilde{\tau}(\mathbf{x})}(\mathbf{x}), 0, \mathcal{G}_I(\pi_{x,y} \Phi_{\tilde{\tau}(\mathbf{x})}(\mathbf{x}), 0)).$$

**Corollary 55.** *From the time reversing symmetry (33) and Lemma 54 we obtain*

$$\mathcal{S}(N^T(r)) \xleftarrow{\tilde{f}^k} \mathcal{S}(N^T(\bar{r}, r)).$$

Let us now consider h-sets on  $\Sigma = \{\phi = 0\}$  of the form (see Figure 10)

$$\begin{aligned} M(\alpha, \beta) &= \{(x, y) : |x - y| \leq L(x + y), x + y \in [\alpha, \beta]\} \\ M^r(\alpha, \beta) &= M(\alpha, \beta) \cap \{(x, y) : x - y = L(x + y)\}, \\ M^l(\alpha, \beta) &= M(\alpha, \beta) \cap \{(x, y) : x - y = -L(x + y)\}, \\ M^+(\alpha, \beta) &= M(\alpha, \beta) \cap (\{(x, y) : x + y = \alpha\} \cup \{(x, y) : x + y = \beta\}). \end{aligned} \quad (77)$$

**Lemma 56.** *If  $B \in \mathbb{R}$ ,  $B > 0$ , is sufficiently close to zero, then for any  $\alpha < \beta \leq B$  there exists an  $\ell$  (depending on the choice of  $\alpha, \beta$ ) such that*

$$M(\alpha, \beta) \xrightarrow{f^\ell} N(\bar{r}, r).$$

**Proof.** By Proposition 29, if  $\beta < r_*$  (see statement of Proposition 29 for the constant  $r_*$ ) a trajectory starting from  $M^r(\alpha, \beta)$  will enter  $S_{I,L,R}^u$ ; see Figure 10-left. If  $r_*$  is sufficiently small, then the trajectory will enter  $S_{I,L,R}^u \cap \{x - y < \bar{r}\}$ . Moreover, such trajectory will exit  $S_{I,L,R}^u \cap \{x - y \leq r\}$  through  $S_{I,L,R}^u \cap \{x - y = r\}$ . This means that there exists an  $\ell > 0$  such that  $f^\ell(M^r(\alpha, \beta)) \cap N(\bar{r}, r) = \emptyset$ . Moreover,  $f^\ell(M^r(\alpha, \beta))$  will be ‘to the right’, along the coordinate  $x$ , of the set  $N(\bar{r}, r)$  so the second condition from (61) in the definition of the covering will be fulfilled.

The set  $M^l(\alpha, \beta)$  gets mapped outside and above (with respect to  $y$ ) the set  $\mathcal{S}(S_{I,L,R}^u)$ ; see Figure 10. By the symmetry of the system a trajectory which starts from  $M^l(\alpha, \beta)$  will never re-enter  $\mathcal{S}(S_{I,L,R}^u \cup S_{I,R_1,R_2,\varepsilon})$ , so  $f^\ell(M^l(\alpha, \beta))$  will always have the  $y$  coordinate bigger than zero. This means that topologically the set  $f^\ell(M^l(\alpha, \beta))$  is to the left of  $N(\bar{r}, r)$  along the  $x$  coordinate (see Figure 10-right). Therefore the first condition from (61) in the definition of the covering will be fulfilled.

Any point from  $M(\alpha, \beta)$  that enters  $S_{I,L,R}^u$  does so through  $\{x - y < \bar{r}\}$ . Once a trajectory enters, it can not exit through  $\partial S_{I,L,R}^u \setminus \{q = R\}$ , so

$$f^\ell(M^r(\alpha, \beta)) \cap N^+(\bar{r}, r) = \emptyset,$$

which means that condition (63) definition of the covering is fulfilled. ■

Observe that

$$M(\bar{r}, r) = \mathcal{S}(N^T(\bar{r}, r)).$$

**Lemma 57.** *Let  $\bar{r}, r > 0$  be fixed. For every  $\beta > 0$  there exist  $m > 0$  and  $\alpha > 0$  (the  $m$  and  $\alpha$  depend on the choice of  $\bar{r}, r, \beta$ ) such that*

$$M(\bar{r}, r) \xrightarrow{f^m} M(\alpha, \beta) \tag{78}$$

**Proof.** From the symmetry of the system, any point in  $M^-(\bar{r}, r) = M^l(\bar{r}, r) \cup M^r(\bar{r}, r)$  will flow out of  $\mathcal{S}(S_{I,L,R}^u)$ . From the definition of  $f$ , if  $\mathbf{x} \in M^-(\bar{r}, r)$  then  $f^i(\mathbf{x})$  will not return to  $\mathcal{S}(S_{I,L,R}^u)$ . Moreover, the images of the components of  $M^-(\bar{r}, r)$  will remain on different sides of  $\mathcal{S}(S_{I,L,R}^u \cup S_{I,R_1,R_2,\varepsilon})$ . This implies (61) for any choice of  $\alpha, \beta$ .

As long as the flow which starts from  $\mathbf{x} \in M(\bar{r}, r)$  remains in  $\mathcal{S}(S_{I,L,R}^u)$ , it approaches  $\Lambda_I$  (This follows from the outflowing property in  $S_{I,L,R}^u$  and the symmetry of the system). Therefore, by compactness of  $M(\bar{r}, r)$ , one can find a sufficiently large  $m$  so that if  $\mathbf{x} \in M(\bar{r}, r)$  and  $f^m(\mathbf{x}) \in \mathcal{S}(S_{I,L,R}^u)$  then  $f^m(\mathbf{x}) \in \{x + y < \beta\}$ . Let us fix such  $m$ . We can now choose  $\alpha > 0$  sufficiently small so that if  $\mathbf{x} \in M(\bar{r}, r)$  and  $f^m(\mathbf{x}) \in \mathcal{S}(S_{I,L,R}^u)$  then  $f^m(\mathbf{x}) \in \{x + y > \alpha\}$ . We have thus established (78). ■

We are now ready to prove Theorem 1.

**Proof of Theorem 1.** Let us start by choosing sufficiently small  $0 < \bar{r} < r$  so that we have

$$N(\bar{r}, r) \xrightarrow{f^k} N(r) \xrightarrow{f_1} N_1 \xrightarrow{f_0} N_0. \tag{79}$$

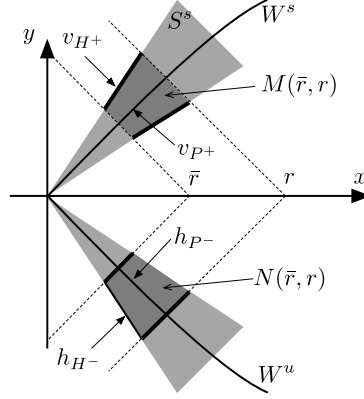


Figure 11: The horizontal discs  $h_{P^-}$ ,  $h_{H^-}$  and the vertical discs  $v_{P^+}$  and  $v_{H^+}$ .

This can be done by Lemmas 47, 51, 54. We choose  $r$  and  $\bar{r}$  to be small enough, so that  $\pi_{q,p}N(\bar{r}, r) \subset [-\sqrt{r^*}, \sqrt{r^*}]^2$  where  $r^*$  is the constant from Proposition 29. We also choose  $r$  to be small enough so that

$$h_{P^-} := W_{\Lambda_I}^u \cap \Sigma \cap N(\bar{r}, r)$$

is a horizontal disc in  $N(\bar{r}, r)$  and that

$$v_{P^+} := W_{\Lambda_I}^s \cap \Sigma \cap M(\bar{r}, r)$$

is a vertical disc in  $M(\bar{r}, r)$ ; see Figure 11. The  $\bar{r}$  and  $r$  will remain fixed throughout the proof.

We also define a horizontal disc  $h_{H^-}$  in  $N(\bar{r}, r)$  to be the lower boundary of  $N(\bar{r}, r)$  and define the vertical disc  $v_{H^+}$  in  $M(\bar{r}, r)$  to be the left boundary of  $M(\bar{r}, r)$ ; see Figure 11.

All orbits which pass through  $|h_{P^-}|$  converge backwards in time to  $\Lambda_I$ , hence they belong to  $P^-$ . Similarly, orbits which pass through  $|v_{P^+}|$  belong to  $P^+$ . By Item 2 of Proposition 29, orbits which pass through  $|v_{H^+}|$  belong to  $H^+$ . By the symmetry of the system, orbits that pass through  $|h_{H^-}|$  belong to  $H^-$ . We will use the discs  $v_{H^+}$ ,  $h_{H^-}$ ,  $v_{P^+}$  and  $h_{P^-}$  to obtain orbits from  $H^-$  or  $P^-$  to  $H^+$  or  $P^+$ .

The idea for the proof of  $OS^\pm$  is to consider a sequence  $\{\beta_i\}$  with  $\beta_i > 0$ , and to construct a sequence of coverings, which will successively link  $N_0$  with  $M(\alpha_i, \beta_i)$  (each time returning back to  $N_0$ ), for suitably chosen  $\alpha_i$ . Below we will show how such link can be constructed for a fixed  $\beta$ . Later on in the proof this construction will be repeated for each  $\beta_i$  from  $\{\beta_i\}$ .

By Corollaries 48, 52, 55, there exists

$$N_0 \xleftarrow{\tilde{f}_0} \mathcal{S}(N_1^T) \xleftarrow{\tilde{f}_1} \mathcal{S}(N^T(r)) \xleftarrow{\tilde{f}^k} \mathcal{S}(N^T(\bar{r}, r)) = M(\bar{r}, r). \quad (80)$$

For a given small  $\beta$ , by Lemma 57 there exists an  $\alpha = \alpha(\beta) > 0$  and  $m = m(\beta) \in \mathbb{N}$  such that

$$M(\bar{r}, r) \xrightarrow{f^m} M(\alpha, \beta). \quad (81)$$

By Lemma 56, there exists a  $\ell = \ell(\alpha, \beta)$  such that

$$M(\alpha, \beta) \xrightarrow{f^\ell} N(\bar{r}, r). \quad (82)$$

For the above choice of  $\alpha, m$  and  $\ell$ , combining (79–82) we obtain

$$\begin{aligned} N_0 \xleftarrow{\tilde{f}_0} \mathcal{S}(N_1^T) \xleftarrow{\tilde{f}_1} \mathcal{S}(N^T(r)) \xleftarrow{\tilde{f}^k} M(\bar{r}, r) \xrightarrow{f^m} \\ \xrightarrow{f^m} M(\alpha, \beta) \xrightarrow{f^\ell} N(\bar{r}, r) \xrightarrow{f^k} N(r) \xrightarrow{f_1} N_1 \xrightarrow{f_0} N_0. \end{aligned} \quad (83)$$

To simplify the notation, let us denote such sequence of coverings by

$$N_0 \xrightarrow[\beta]{} N_0. \quad (84)$$

In the notation, by writing the  $\beta$  we emphasize that (83) includes the set  $M(\alpha, \beta)$ . This will play an important role in our arguments. Whenever we write (84), we will understand this as choosing the  $\beta$  first, and then the  $\alpha, m$  and  $\ell$  in (83) are chosen so that the sequence of coverings is ensured. The important issue is that we can construct such sequence for an arbitrarily small  $\beta$ .

Let us now introduce the following sequences of coverings:

( $H^-$ ) The sequence that will lead to hyperbolic motions in backward time, which we shall denote as ( $H^-$ ), is

$$N(\bar{r}, r) \xrightarrow{f^k} N(r) \xrightarrow{f_1} N_1 \xrightarrow{f_0} N_0. \quad (85)$$

( $P^-$ ) We will also use the sequence (85) for the proof of parabolic motions in backward time, which we denote by ( $P^-$ ).

( $H^+$ ) The sequence that will lead to hyperbolic motions in forward time, which we shall denote as ( $H^+$ ),

$$N_0 \xleftarrow{\tilde{f}_0} \mathcal{S}(N_1^T) \xleftarrow{\tilde{f}_1} \mathcal{S}(N^T(r)) \xleftarrow{\tilde{f}^k} M(\bar{r}, r). \quad (86)$$

( $P^+$ ) We will also use the sequence (86) for the proof of parabolic motions in forward time, denoted by ( $P^+$ ).

( $B^-$ ) The sequence that will lead to bounded motions in backward time

$$\cdots \xrightarrow[r]{} N_0 \xrightarrow[r]{} N_0 \xrightarrow[r]{} N_0. \quad (87)$$

(Above coverings are expressed in our simplified notation (84) with  $\beta = r$ .)

( $B^+$ ) The sequence that will lead to bounded motions in forward time:

$$N_0 \xrightarrow[r]{} N_0 \xrightarrow[r]{} N_0 \xrightarrow[r]{} \cdots. \quad (88)$$

( $OS^-$ ) For a fixed sequence  $\dots, \beta_{-3}, \beta_{-2}, \beta_{-1} \in \mathbb{R}$  we consider a sequence of coverings

$$\dots \xrightarrow{\beta_{-3}} N_0 \xrightarrow{\beta_{-2}} N_0 \xrightarrow{\beta_{-1}} N_0.$$

(These coverings are expressed in our simplified notation (84).)

( $OS^+$ ) For a fixed sequence  $\beta_0, \beta_1, \beta_2, \dots \in \mathbb{R}$  we consider a sequence of coverings

$$N_0 \xrightarrow{\beta_0} N_0 \xrightarrow{\beta_1} N_0 \xrightarrow{\beta_2} \dots$$

To obtain orbits from  $X^- \cap Y^+$  for  $X, Y \in \{H, P, B, OS\}$  we combine sequences ( $X^-$ ) with ( $Y^+$ ).

For example, to obtain an orbit from  $H^- \cap P^+$  we glue ( $H^-$ ) with ( $P^+$ ) which gives

$$N(\bar{r}, r) \xrightarrow{f^k} N(r) \xrightarrow{f_1} N_1 \xrightarrow{f_0} \textcircled{N_0} \xleftarrow{\tilde{f}_0} \mathcal{S}(N_1^T) \xleftarrow{\tilde{f}_1} \mathcal{S}(N^T(r)) \xleftarrow{\tilde{f}^k} M(\bar{r}, r).$$

The circle indicates where the sequences are glued. Now, by Theorem 44 we obtain an orbit starting from  $|h_{H^-}|$  which goes to  $|v_{P^+}|$ , which proves that  $H^- \cap P^+ \neq \emptyset$ .

As another example we will show how to obtain an orbit from  $B^- \cap OS^+$ . By gluing ( $B^-$ ) with ( $OS^+$ ), we obtain

$$\dots \xrightarrow{r} N_0 \xrightarrow{r} N_0 \xrightarrow{r} \textcircled{N_0} \xrightarrow{\beta_0} N_0 \xrightarrow{\beta_1} N_0 \xrightarrow{\beta_2} \dots \quad (89)$$

We can take the sequence  $\{\beta_i\}$  used in ( $OS^+$ ) to converge to zero. By Item 3 of Corollary 45, from (89) we obtain an orbit which passes through this sequence. We clearly have bounded motions in backward time. The trajectory going forwards in time will be making alternating visits between  $N_0$  and  $M(\alpha_i, \beta_i)$  for  $i \in \mathbb{N}$ . The smaller the  $\beta_i$ , the closer are the sets  $M(\alpha_i, \beta_i)$  to  $\Lambda_I$ ; which means that the further they are from the origin for the original system associated to (28). This means that the orbit belongs to  $OS^+$ .

All other types of motions follow from mirror arguments: gluing of sequences ( $X^-$ ) and ( $Y^+$ ), for  $X, Y \in \{H, P, B, OS\}$  and using Theorem 44 or Corollary 45.

The bound for  $r_0$  follows from computing

$$\{r = 2/x^2 \mid x \in \pi_x N_0\} = [0.4999086, 0.5001915].$$

By Theorem 44 we obtain a periodic orbit passing through a sequence  $N_0 \xrightarrow{r} N_0$ . Such orbit passes through the set  $N(\bar{r}, r)$ . The smaller the  $r$  the further (in the original coordinates of the system) is such set from the origin. Since we can take  $r$  as small as we wish, we can obtain periodic orbits which reach as far from the origin as we wish. The orbits also pass through  $N_0$  so they pass  $r_0$  close to the origin.

The total computation time for the computer assisted part of the proof (i.e. for the validation of the sector, the extended sector and for the validation of  $N_1 \xrightarrow{f_0} N_0$ ) was 155 seconds, running on a single thread on a standard laptop.

This concludes our proof. ■

## 7. Appendix

Here we write the properties of the local Brouwer degree [27]. The *local Brouwer degree* of a continuous map  $f : \mathbb{R}^n \rightarrow \mathbb{R}^n$  at some point  $c \in \mathbb{R}^n$ ,  $n > 0$ , in a set  $U \subset \mathbb{R}^n$  is a certain number. Suppose that

$$\text{the set } f^{-1}(c) \cap U \text{ is compact.} \quad (90)$$

Then the *local Brouwer degree of  $f$  at  $c$  in the set  $U$*  is well defined. We denote it by  $\deg(f, U, c)$ .

If  $\bar{U} \subset \text{dom}(f)$  and  $\bar{U}$  is compact, then (90) follows from the condition

$$c \notin f(\partial U). \quad (91)$$

Let us summarize the properties of the local Brouwer degree.

**Degree is an integer.**

$$\deg(f, U, c) \in \mathbb{Z}. \quad (92)$$

**Solution property.**

$$\text{If } \deg(f, U, c) \neq 0, \text{ then there exists } x \in U \text{ with } f(x) = c. \quad (93)$$

**Homotopy property.** Let  $H : [0, 1] \times U \rightarrow \mathbb{R}^n$  be continuous. Suppose that

$$\bigcup_{\lambda \in [0, 1]} H_\lambda^{-1}(c) \cap U \text{ is compact.} \quad (94)$$

Then

$$\forall \lambda \in [0, 1] \quad \deg(H_\lambda, U, c) = \deg(H_0, U, c). \quad (95)$$

If  $[0, 1] \times \bar{U} \subset \text{dom}(H)$  and  $\bar{U}$  is compact, then (94) follows from the following condition

$$c \notin H([0, 1], \partial U). \quad (96)$$

**Local degree for affine maps.** Suppose that  $f(x) = A(x - x_0) + c$ , where  $A$  is a linear map and  $x_0 \in \mathbb{R}^n$ . If the equation  $A(x) = 0$  has no nontrivial solutions (i.e. if  $Ax = 0$ , then  $x = 0$ ) and  $x_0 \in U$ , then

$$\deg(f, U, c) = \text{sgn}(\det A). \quad (97)$$

## References

- [1] J. Chazy, [Sur l'allure du mouvement dans le problème des trois corps quand le temps croît indéfiniment](#), Ann. Sci. École Norm. Sup. (3) 39 (1922) 29–130.  
URL [http://www.numdam.org/item?id=ASENS\\_1922\\_3\\_39\\_29\\_0](http://www.numdam.org/item?id=ASENS_1922_3_39_29_0)
- [2] V. Arnold, V. Kozlov, A. Neishtadt, Dynamical Systems III, Vol. 3 of Encyclopaedia Math. Sci., Springer, Berlin, 1988.
- [3] K. Sitnikov, The existence of oscillatory motions in the three-body problems, Soviet Physics. Dokl. 5 (1960) 647–650.

- [4] J. Llibre, C. Simó, [Some homoclinic phenomena in the three-body problem](#), *J. Differential Equations* 37 (3) (1980) 444–465. doi:10.1016/0022-0396(80)90109-6.  
URL [http://dx.doi.org/10.1016/0022-0396\(80\)90109-6](http://dx.doi.org/10.1016/0022-0396(80)90109-6)
- [5] M. Guardia, P. Martín, T. M. Seara, [Oscillatory motions for the restricted planar circular three body problem](#), *Invent. Math.* 203 (2) (2016) 417–492. doi:10.1007/s00222-015-0591-y.  
URL <https://doi.org/10.1007/s00222-015-0591-y>
- [6] V. M. Alekseev, Quasirandom dynamical systems. I, II, III, *Math. USSR* 5,6,7.
- [7] J. Moser, *Stable and random motions in dynamical systems*, Princeton University Press, Princeton, N. J., 1973, with special emphasis on celestial mechanics, Hermann Weyl Lectures, the Institute for Advanced Study, Princeton, N. J., *Annals of Mathematics Studies*, No. 77.
- [8] J. Llibre, C. Simó, [Oscillatory solutions in the planar restricted three-body problem](#), *Math. Ann.* 248 (2) (1980) 153–184. doi:10.1007/BF01421955.  
URL <http://dx.doi.org/10.1007/BF01421955>
- [9] M. Guardia, J. Paradela, T. M. Seara, C. Vidal, [Symbolic dynamics in the elliptic isosceles restricted three body problem](#), preprint (2020).  
URL <https://arxiv.org/abs/2012.04696>
- [10] R. Moeckel, [Symbolic dynamics in the planar three-body problem](#), *Regul. Chaotic Dyn.* 12 (5) (2007) 449–475. doi:10.1134/S1560354707050012.  
URL <http://dx.doi.org/10.1134/S1560354707050012>
- [11] M. Guardia, T. M. Seara, P. Martín, L. Sabbagh, [Oscillatory orbits in the restricted elliptic planar three body problem](#), *Discrete Contin. Dyn. Syst.* 37 (1) (2017) 229–256. doi:10.3934/dcds.2017009.  
URL <https://doi.org/10.3934/dcds.2017009>
- [12] T. M. Seara, J. Zhang, [Oscillatory orbits in the restricted planar four body problem](#), *Nonlinearity* 33 (12) (2020) 6985–7015. doi:10.1088/1361-6544/abaf5f.  
URL <https://doi.org/10.1088/1361-6544/abaf5f>
- [13] J. Galante, V. Kaloshin, [Destruction of invariant curves in the restricted circular planar three-body problem by using comparison of action](#), *Duke Math. J.* 159 (2) (2011) 275–327. doi:10.1215/00127094-1415878.  
URL <http://dx.doi.org/10.1215/00127094-1415878>
- [14] J. Galante, V. Kaloshin, [The method of spreading cumulative twist and its application to the restricted circular planar three body problem](#), preprint, available at <http://www.terpconnect.umd.edu/~vkaloshi> (2010).
- [15] J. Galante, V. Kaloshin, [Destruction of invariant curves using the ordering condition](#), preprint, available at <http://www.terpconnect.umd.edu/~vkaloshi> (2010).
- [16] R. McGehee, [A stable manifold theorem for degenerate fixed points with applications to celestial mechanics](#), *J. Differential Equations* 14 (1973) 70–88.
- [17] V. K. Melnikov, [On the stability of the center for time periodic perturbations](#), *Trans. Moscow Math. Soc.* 12 (1963) 1–57.
- [18] S. Smale, [Diffeomorphisms with many periodic points](#), in: *Differential and Combinatorial Topology (A Symposium in Honor of Marston Morse)*, Princeton Univ. Press, Princeton, N.J., 1965, pp. 63–80.
- [19] P. Zgliczyński, M. Gidea, [Covering relations for multidimensional dynamical systems](#), *J. Differential Equations* 202 (1) (2004) 32–58. doi:10.1016/j.jde.2004.03.013.  
URL <https://doi.org/10.1016/j.jde.2004.03.013>
- [20] R. Easton, [Isolating blocks and symbolic dynamics](#), *J. Differential Equations* 17 (1975) 96–118. doi:10.1016/0022-0396(75)90037-6.
- [21] R. Easton, [Homoclinic phenomena in hamiltonian systems with several degrees of freedom](#), *J. Differential Equations* 29 (1978) 241–252. doi:10.1016/0022-0396(78)90123-7.
- [22] G. Dahlquist, [Stability and error bounds in the numerical integration of ordinary differential equations](#), Inaugural dissertation, University of Stockholm, Almqvist & Wiksells Boktryckeri AB, Uppsala, 1958.
- [23] S. M. Lozinskiĭ, [Error estimate for numerical integration of ordinary differential equations. I](#), *Izv. Vysš. Učebn. Zaved. Matematika* 1958, no. 5 (6), 52–90; 1959 (5 (12)) (1959) 222.
- [24] M. J. Capiński, P. Zgliczyński, [Beyond the Melnikov method: a computer assisted approach](#), *J. Differential Equations* 262 (1) (2017) 365–417. doi:10.1016/j.jde.2016.09.032.  
URL <https://doi.org/10.1016/j.jde.2016.09.032>
- [25] S. M. Rump, [Verification methods: rigorous results using floating-point arithmetic](#), *Acta Numer.* 19 (2010) 287–449. doi:10.1017/S096249291000005X.  
URL <https://doi.org/10.1017/S096249291000005X>

- [26] D. Wilczak, P. Zgliczyński, [Topological method for symmetric periodic orbits for maps with a reversing symmetry](#), *Discrete Contin. Dyn. Syst.* 17 (3) (2007) 629–652. doi:10.3934/dcds.2007.17.629.  
URL <https://doi.org/10.3934/dcds.2007.17.629>
- [27] N. G. Lloyd, *Degree theory*, Cambridge University Press, Cambridge-New York-Melbourne, 1978, *Cambridge Tracts in Mathematics*, No. 73.